J Physiol (2003), **549.1**, *pp.* 37–56
DOI: 10.1113/jphysiol.2002.029546

www.jphysiol.org

Journal of Physiology

Gastrointestinal-projecting neurones in the dorsal motor nucleus of the vagus exhibit direct and viscerotopically organized sensitivity to orexin

Gintautas Grabauskas and Hylan C. Moises

Department of Physiology and Neuroscience Program, University of Michigan Medical School, Ann Arbor, MI 48109-0622, USA

Orexin (hypocretin)-containing projections from lateral hypothalamus (LH) are thought to play an important role in the regulation of feeding behaviour and energy balance. In rodent studies, central administration of orexin peptides increases food intake, and orexin neurones in the LH are activated by hypoglycaemia during fasting. In addition, administration of orexins into the fourth ventricle or the dorsal motor nucleus of the vagus (DMV) has been shown to stimulate gastric acid secretion and motility, respectively, via vagal efferent pathways. In this study, whole-cell recordings were obtained from DMV neurones in rat brainstem slices to investigate the cellular mechanism(s) by which orexins produce their gastrostimulatory effects. To determine whether responsiveness to orexins might be differentially expressed among distinct populations of preganglionic vagal motor neurones, recordings were made from neurones whose projections to the gastrointestinal tract had been identified by retrograde labelling following apposition of the fluorescent tracer DiI to the gastric fundus, corpus or antrum/pylorus, the duodenum or caecum. Additionally, the responses of neurones to orexins were compared with those produced by oxytocin, which acts within the DMV to stimulate gastric acid secretion, but inhibits gastric motor function. Bath application of orexin-A or orexin-B (30–300 nM) produced a slow depolarization, accompanied by increased firing in 47 of 102 DMV neurones tested, including 70 % (30/43) of those that projected to the gastric fundus or corpus. In contrast, few DMV neurones that supplied the antrum/pylorus (3/13), duodenum (4/18) or caecum (1/13) were responsive to these peptides. The depolarizing responses were concentration dependent and persisted during synaptic isolation of neurones with TTX or Cd^{2+}, indicating they resulted from activation of postsynaptic orexin receptors. They were also associated with a small increase in membrane resistance, and in voltage-clamp recordings orexin-A induced an inward current that reversed near the estimated equilibrium potential for K^+, indicating the depolarization was due in large part to a reduction in K^+ conductance. Orexins did not affect synaptically evoked excitation, but did reduce membrane excitability in a subset of gastric-projecting DMV neurones by enhancing GABA-mediated synaptic input. Lastly, although many DMV neurones responded to orexins and oxytocin with excitation, for the most part these peptides modulated excitability of distinct populations of gastric-projecting vagal motor neurones. These results indicate that orexins act preferentially within the DMV to directly excite vagal motor neurones that project to gastric fundus and corpus. In this way, release of endogenous orexins from descending hypothalamic projections into the DMV may mediate the increase in gastric acid secretion and motor activity associated with the cephalic phase of feeding.

(Received 19 August 2002; accepted after revision 5 March 2003; first published online 4 April 2003)
Corresponding author H. C. Moises: Department of Physiology, University of Michigan Medical School, Ann Arbor, MI 48109-0622, USA. E-mail: moises@umich.edu

The orexins, also called hypocretins (Sakurai *et al.* 1998; de Lecea *et al.* 1998), are a novel pair of hypothalamic neuropeptides implicated in the regulation of energy balance and arousal (see Willie *et al.* 2001; Sutcliffe & de Lecea, 2002 for reviews). Initial excitement about these peptides derived from the finding that both forms of orexin (orexin-A and orexin-B) are synthesized exclusively by neurones located in the lateral hypothalamic area (LHA) and adjacent perifornical region, areas classically implicated in the control of mammalian feeding behaviour (Sakurai *et al.* 1998; Peyron *et al.* 1998; Date *et al.* 1999). Additionally, it was shown that intracerebroventricular administration of orexins or injection of these peptides directly into specific hypothalamic loci produced dose-dependent increases in food intake in rats (Sakurai *et al.* 1998; Dube *et al.* 1999), whereas administration of orexin antibodies (Yamada *et al.* 2000) inhibited feeding in fasted animals. Moreover, the hypothalamic expression of

prepro-orexin mRNA is increased by fasting (Sakurai *et al.* 1998) and after acute hypoglycaemia when food is withheld (Cai *et al.* 1999), while conversely down-regulated in genetically obese *ob* and *db* mice (Yamamoto *et al.* 1999). These data, together with more recent findings that orexin neurones show robust activation to hypoglycemic challenge in fasted rats (Cai *et al.* 2001), suggest that orexins may be involved in the acute control of glucostatic feeding in addition to homeostatic mechanisms that regulate energy balance.

Orexin immunoreactive axonal fibres are widely distributed throughout the neuraxis, with the most prominent projections found in hypothalamic and brainstem nuclei known to be important in feeding-related behaviours or maintenance of wakefulness (Peyron *et al.* 1998; Horvath *et al.* 1999*a*,*b*). In addition, orexin-containing nerve fibres and specific receptors for orexins are found in moderate to high density in many autonomic centres in rat brainstem and spinal cord, including the dorsal vagal complex (DVC) in the medulla (Harrison *et al.* 1999; Krowicki *et al.* 2002). The DVC consists of the nucleus of the solitary tract (NTS) and dorsal motor nucleus of the vagus (DMV) that together form the hub of a central neural network that provides parasympathetic control over the gastrointestinal (GI) tract and coordinates digestive functions (Gillis *et al.* 1989; Powley *et al.* 1992). The NTS receives various kinds of visceral information from sensory vagal afferents that supply diverse regions of the GI tract, and in turn projects heavily onto preganglionic motor neurones in the DMV that are the major source of parasympathetic innervation to the subdiaphragmatic visceral organs (Gillis *et al.* 1989). These connections provide the neural substrate for a variety of vagovagal reflexes involved in the feedback regulation of GI functions. Moreover, modulation of the vagovagal circuitry within the DVC by descending input from the hypothalamic paraventricular nucleus (PVN) and lateral hypothalamic area (LHA) constitutes the primary means whereby higher centres exert a direct influence over gastric and pancreatic secretion, as well as stomach and small intestinal motility (Gillis *et al.* 1989; Loewy, 1990; Bernardis & Bellinger, 1996).

The possibility that orexin-containing projections to the DVC play a role in the central regulation of gastric function was first suggested by Takahashi *et al.* (1999), who demonstrated that administration of orexin-A into the fourth ventricle stimulates gastric acid secretion in conscious rats. The stimulatory effect of orexin-A on acid secretion was blocked by atropine and abolished in vagotomized animals, indicating that it was dependent upon increases in vagal efferent nerve activity. Additionally, Hornby and co-workers have shown in anaesthetized rat that microinjection of orexin-A or -B into the DMV, but not into surrounding areas, increases gastric tone and stimulates motility via a vagal dependent mechanism (Krowicki *et al.* 2002). These data raise the possibility that release of orexins within the DMV may mediate the cephalic phase of normal digestive functions, characterized by increased acid secretion and gastric contractions, which occurs in anticipation of feeding (Powley, 2000).

Recent immunohistochemical studies and results from *in situ* hybrization experiments indicate that orexin-1 receptors are highly expressed in neurones of the rat DMV (Marcus *et al.* 2001; Krowicki *et al.* 2002). Moreover, recordings obtained in rat medullary slices revealed that orexins directly depolarize a fraction (approximately 30 %) of DMV neurones (Hwang *et al.* 2001), including some that were identified as preganglionic parasympathetic neurones based on their retrograde labelling following intraperitoneal injection of Fluorogold. These data provide a cellular basis for the vagally mediated increase in gastric acid secretion produced following administration of orexin-A into the fourth ventricle (Takahashi *et al.* 1999). Similarly, the stimulation of gastric motor function produced by microinjection of orexins into the DMV could arise largely from activation of preganglionic parasympathetic neurones providing excitatory cholinergic innervation to the stomach. Nevertheless, the DMV consists of a heterogeneous population of neurones (Berthoud *et al.* 1991; Krowicki & Hornby, 1995), including a number of functionally distinct groups of abdominal vagal efferent neurones distinguished according to their neurochemical phenotype, specific site of innervation within the GI tract, and/or pattern of connectivity with excitatory or inhibitory postganglionic motor neurones. Accordingly, it is important to have information about the site of projection of the DMV neurone under study if one is to succeed in relating cellular effects observed *in vitro* to the physiological functions of individual vagal efferent neurones. It should also be mentioned that orexins have been shown to produce a variety of cellular effects in many different types of target neurones, typically producing direct depolarization, but also acting presynaptically to modulate synaptic input (van den Pol *et al.* 1998; Kirchgessner & Liu, 1999; Grudt *et al.* 2002; Liu *et al.* 2002). Although studies by Hwang *et al.* (2001) indicate that orexins directly excite a group of preganglionic parasympathetic DMV neurones, the possibility that orexins also regulate their activity indirectly by modulating synaptic transmission in the DMV remains to be determined.

In the present study, whole-cell recordings were obtained in rat medullary slices to determine the effects of orexin-A and orexin-B on the intrinsic membrane properties and synaptically evoked responses of retrogradely labelled DMV neurones that project either to the gastric fundus, corpus, antrum/pylorus, duodenum or caecum. By correlating the response to orexins in individual DMV

neurones with their site of projection in the GI tract, we sought to determine whether sensitivity to these peptides is expressed preferentially in gastric-projecting vagal neurones or distributed ubiquitously, including among DMV neurones that project to proximal or distal portions of the intestine. The electrophysiological effects of orexin-A were also compared with the responses produced by oxytocin (OT) in many of the same DMV neurones. Earlier studies have established that OT-containing neurones of the PVN provide the major source of descending hypothalamic input to the DMV (Swanson & Kuypers, 1980; Rinaman, 1998), and OT has been shown to evoke a slow depolarization in many gastric-related vagal neurones (Dubois-Dauphin *et al.* 1992). In addition, OT acts via a vagal-dependent mechanism to stimulate gastric acid secretion (Rogers & Hermann, 1985, 1987), similar to orexin-A, whereas it inhibits gastric contractility tonically or when microinjected directly into the DMV (Rogers & Hermann, 1987; Flanagan *et al.* 1992). Based on these data, we hypothesized that orexins and OT might exert their opposing effects on gastric motor activity by acting selectively or in a differential manner to modulate the excitability of 'functionally' distinct groups of gastric-related vagal motor neurones. The corollary hypothesis was also examined, that some gastric-related DMV neurones will be directly excited by orexin-A and OT, providing the cellular substrate by which both types of hypothalamic peptidergic input stimulate gastric acid secretion. A preliminary account of these data has been presented previously (Grabauskas & Moises, 2001).

METHODS

All procedures were performed in accordance with NIH guidelines and with the approval of the Animal Care and Utilization Committee of The University of Michigan, Ann Arbor, MI, USA.

Retrograde labelling

Sprague-Dawley rats (10–12 days olds) of either sex were anaesthetized with a 4% mixture of 2-bromo-2-chloro-1,1,1-trifluorethane (halothane) in air, delivered at 500 ml min^{-1} via a vaporizer (Fluotec-3, Fraser Harlake, NY, USA). The depth of anaesthesia was checked by lack of withdrawal reflex to toe pinch before beginning surgery and maintained constant throughout all surgical procedures by placing the head of the rat in a custom-made chamber through which a reduced halothane (1.0–1.5% in air) mixture was delivered. The abdominal area was shaved and cleaned with 70% ethanol, and an abdominal laparotomy was performed. Crystals of the retrograde tracer 1,1′-dioctadecyl-3,3,3′,3-tetramethylindocarbocyanine perchlorate (DiI; Molecular Probes, Eugene, OR, USA) were applied to a single region of the GI tract per rat, according to procedures described by Browning *et al.* (1999). Dye was deposited either to the greater curvature of the gastric fundus or corpus, to the antrum/pylorus, intestinal duodenum (anti-mesenteric border at the level of the bifurcation of the hepatic and pancreatico-duodenal arteries) or the caecum (at the level of the ileo-caecal junction). To confine the dye to the site of application, crystals of DiI were embedded in a fast hardening epoxy resin that was allowed to harden for approximately 5 min. This was followed by washing of the surgical area with warm sterile saline and blotting of any excess solution with cotton swabs. The wound was then closed with nylon sutures (4-0), and the animal allowed to recover for 8–15 days prior to being killed for electrophysiological study. In 13 experiments the retrograde tracer DiO (Molecular Probes) was also applied to a region distinct from that which received application of DiI (DiI on fundus and DiO on corpus, $n = 4$; DiI on corpus and DiO on duodenum, $n = 4$; DiI on corpus and DiO on antrum/pylorus, $n = 3$; DiI on duodenum and DiO on caecum, $n = 2$)

Brain slice preparation

Coronal tissue slice preparations of rat brainstem were prepared according to procedures described in detail by Browning *et al.* (1999). Briefly, rats were decapitated using a small laboratory animal guillotine and the whole brain, including the brainstem, was rapidly removed and placed in ice-cold physiological saline consisting of (mM): NaCl, 124; KCl, 2.5; $CaCl_2$, 2.5; $MgSO_4$, 1.3; $NaHCO_3$, 26; NaH_2PO_4, 1.25; and glucose, 10, gassed with 95% O_2–5% CO_2 and adjusted to pH 7.3. The cerebellum was removed and the brainstem transected at the level of the pons and again at a point several millimetres caudal to the calamus scriptorius (defined by the caudal-most part of the area postrema). Using a Vibratome, three to four coronal slices (200 μm-thick) containing the DVC were cut and placed in a holding chamber, containing physiological saline maintained at room temperature and continually gassed with 95% O_2–5% CO_2. The slices were incubated for at least 1 h prior to electrophysiological study. A single slice was then transferred to a custom-designed recording chamber (volume ~500 μl), where it was continuously perfused (1–2 ml min^{-1}) under submersion with oxygenated physiological saline (Krebs solution). Slices were normally maintained at room temperature (most current clamp recordings) or else perfused with Krebs solution prewarmed to 34°C for recording of postsynaptic membrane currents under voltage clamp. Recording at the higher temperature had the desired effect of increasing the amplitude and rate of activation of the evoked currents, but had no appreciable effect on responses produced by orexins or OT. Therefore, results obtained under these two conditions have been pooled and are presented together.

Electrophysiological recordings

Prior to electrophysiological recording, retrogradely labelled DMV neurones were identified using a Nikon E600FN microscope equipped with TRITC epifluorescence filters. Once a labelled neurone was identified, its location in the slice was confirmed under brightfield illumination using DIC (Nomarksi) optics. Electrodes for stimulating and recording were placed into position under visual guidance. Unless otherwise indicated, recordings were performed in neurones that were unequivocally identified as labelled with DiI.

Whole-cell patch-clamp recordings were performed using patch pipettes (5–6 MΩ) fashioned from 1.5 mm o.d. borosilicate filament glass and filled with a solution containing (mM): potassium gluconate, 135; KCl, 10; Hepes, 10; EGTA, 10; $MgCl_2$, 1.0; $CaCl_2$, 1.0; ATP, 2.0; GTP, 0.5. In some experiments, CsCl (145 mM) was substituted for potassium salts in the pipette solution to examine for effects of blockade of voltage-dependent K^+ conductances on membrane responses to orexins. Recordings of spontaneous and miniature IPSCs (mIPSCs) were made with a pipette solution that contained 135 mM KCl in place of potassium gluconate. Under these conditions, the amplitudes of IPSCs and mIPSCs are enhanced and appear as inward currents when

neurones are clamped at −60 mV, owing to a positive shift in the Cl^- equilibrium potential. All recording solutions were adjusted to pH 7.2–7.3 with KOH and had an osmolarity of 275–292 mosmol l^{-1}. The data were recorded using an Axopach 1D amplifier (Axon Instruments, Union City, CA, USA), filtered at 3 kHz, digitized via a Digidata 1200C interfaced to a Pentium-based microcomputer, stored and later analysed off-line using pCLAMP 8 software (Axon Instrument, Union City, CA, USA). Correction was made for the tip potential (approximately 8 mV) and only those recordings having a series resistance (i.e. pipette + access resistance) < 15 MΩ were used.

Postsynaptic excitatory and inhibitory currents (EPSCs and IPSCs) were evoked by delivering constant current rectangular pulses (0.5 ms duration) via a tungsten bipolar stimulating electrode placed under visual control in the nucleus commissuralis or medialis of the NTS. Single shocks or pairs of stimuli (spaced 100 ms apart) were applied every 30 s, and the stimulus intensity was adjusted to evoke submaximal (~65 % max) excitatory or inhibitory currents that ranged in amplitude from 50 to 300 pA. The criteria for detecting spontaneous synaptic currents were fast rise times (< 1 ms) and exponential decays, with 20 pA (at least twice baseline noise) used as the detection limit for minimum PSC amplitude. Frequencies of spontaneous synaptic events were obtained over continuous periods of recording, lasting from 2 to 5 min, and between 250 and 400 consecutive PSCs were measured for determinations of mean amplitudes.

Drug application

Drugs were applied to the bath in known concentrations via a series of manually operated switching valves. Because of the long duration of effects encountered with orexins or OT, superfusion of peptides was terminated once a plateau effect was observed. When experiments were performed to determine concentration–response relationships, the subsequent superfusion of different concentrations of peptide was randomized and a washout period of at least 30 min was allowed between individual trails. Recordings of spontaneous IPSCs and IPSCs evoked in response to stimulation of the NTS were carried out in the presence of 6-cyano-7-nitroquinoxaline-2,3-dione (CNQX; 20 μM) and 2-amino-5-phosphonovaleric acid (APV; 50 μM) to eliminate contamination by EPSCs. Administration of these antagonists at the concentrations indicated has been shown previously to eliminate spontaneous and evoked glutamatergic synaptic currents in DMV neurones, without affecting GABA-mediated inhibitory synaptic events (Willis *et al.* 1996). Conversely, recordings of stimulation-evoked EPSCs were carried out in the presence of bicuculline methiodide (BMI, 30 μM) or picrotoxin (100 μM) to selectively eliminate spontaneous and evoked GABAergic inhibitory postsynaptic currents (Browning & Travagli, 1999). For all experiments with PSCs, a minimum of 10 control excitatory or inhibitory postsynaptic current responses were obtained prior to application of drug and the effects were assessed using each neurone as its own control, i.e. the results obtained after administration of a receptor antagonist or peptide were compared to those obtained before drug administration.

Data and statistical analysis

Recordings were considered acceptable if the membrane remained stable at the holding potential (usually −60 mV), the resting membrane potential of the neurone was more negative than −50 mV, and the neurone generated overshooting action potentials. The input resistance of recorded neurones was calculated by measuring the amplitude of electrotonic potentials evoked in response to passage of a series of 20 pA constant current pulses (400 ms in duration) through the recording electrode, determined before the onset of any inward rectification. Data are presented in the text as means ± S.E.M. Statistical analysis was performed using Student's paired *t* test and the significance was accepted at the level $P < 0.05$. Group differences in responsiveness to orexins or OT as a function of the GI projection of DMV neurones were determined using the chi-square test. Analysis of PSC frequency and amplitude was conducted with commercially available Mini Analysis software (Synaptosoft, Inc., Decatur, GA, USA). This program detects and measures spontaneous synaptic events according to the amplitude, rate of rise, duration and area under the curve (fc). Statistical comparisons of the extracted amplitude and interspike interval distributions for PSCs were obtained using the nonparametric Kolmogorov–Smirnov test, with a significant difference being set at $P < 0.01$.

Drugs

Orexin-A and Orexin-B were purchased from Bachem (King of Prussia, PA, USA). DiI was obtained from Molecular Probes (Eugene, OR, USA). Tetrodotoxin (TTX) was purchased from Alamone Laboratories (Jerusalem, Israel). Oxytocin, bicucculine methiodide (BMI), picrotoxin, CNQX, APV and all other chemicals were purchased from Sigma-Aldrich-RBI (St Louis, MO, USA).

RESULTS

Membrane properties of DMV neurones

The results are based on recordings obtained from 219 DMV neurones in medullary slices from 98 rats, ranging in age from 18 to 27 days. The vast majority of these recordings ($n = 204$) were from neurones that were retrogradely labelled by application of DiI to the gastric fundus ($n = 50$), corpus ($n = 85$), antrum/pylorus ($n = 24$), duodenum ($n = 27$) or caecum ($n = 18$). Depending on the placement of DiI, four to ten unequivocally labelled neurones could be identified within the DMV in each slice preparation, interspersed among a background of numerous unlabelled cells (Fig. 1). In our labelling technique, applications of DiI were restricted to loci along the greater curvature of the stomach or anti-mesenteric site of the intestine, as these areas contain few or no fibres of passage, but rather vagal nerve terminals (Berthoud *et al.* 1990). Thus, the retrograde labelling of individual somata was likely to be selective for the specific GI region to which application of DiI was made. In addition, in the 13 experiments in which both DiI and DiO were placed on separate regions of the GI tract, double labelling was never observed (i.e. no neurones showed the presence of both DiI and DiO), arguing in favour of the selectivity of our tracing technique (see Fig. 1*B*).

DMV neurones used in this study showed no apparent age-related differences in either their basic electrophysiological properties or responsivess to orexins, and therefore results obtained from neurones examined at days 18 to 27 of maturation have been pooled. In current clamp recordings, retrogradely labelled DMV neurones had a mean resting membrane potential of −56 ± 1.3 mV (range, −54 to −62 mV), mean input resistance of

701 ± 25 MΩ (range, 665 to 790 MΩ), and overshooting action potentials with mean amplitude of 79.2 ± 5.1 mV (range, 74.2 to 82.8 mV) and duration of 3.1 ± 0.2 ms (range, 2.8 to 3.4 ms). These values compare favourably with those reported by Browning *et al.* (1999) for DMV neurones with the corresponding GI projection, although measurements of membrane input resistance were notably higher due to recording at room temperature as opposed to 34 °C (as done in voltage-clamp recordings). Similarly, a large majority (67 %) of the DMV neurones we recorded were spontaneously active, with no significant difference in mean firing rate observed between the different neuronal groups (0.98 ± 0.22 spikes s^{-1}, range 0.1–2 spikes s^{-1}).

Effects of orexin-A and orexin-B in DMV neurones

The electrophysiological effects of orexin-A or orexin-B were examined in current-clamp recordings from 102 DMV neurones, including 87 that were identified as GI-projecting by their labelling with DiI. For these experiments, the membrane potential of the neurone was held at −60 mV by injecting constant current through the recording electrode to prevent spontaneous firing in the absence of peptide. Bath adminstration of orexin-A at a saturating concentration (300 nM) produced excitation in 46 % of the DMV neurones (47 total, including 9/15 unidentified neurones), manifested by a slow membrane depolarization (Fig. 2*A*). In 43 of the neurones in which orexin-A produced depolarization, this was accompanied by a marked increase in spontaneous firing that for the group averaged 2.8 ± 1.1 spikes s^{-1} ($P < 0.05$). Both the orexin-induced depolarization and increase in firing were of prolonged duration, continuing unabated for 15–45 min before returning to control levels following washout of peptide from the bath (Fig. 2*A*). The excitatory effects of orexin-A were also concentration dependent in a

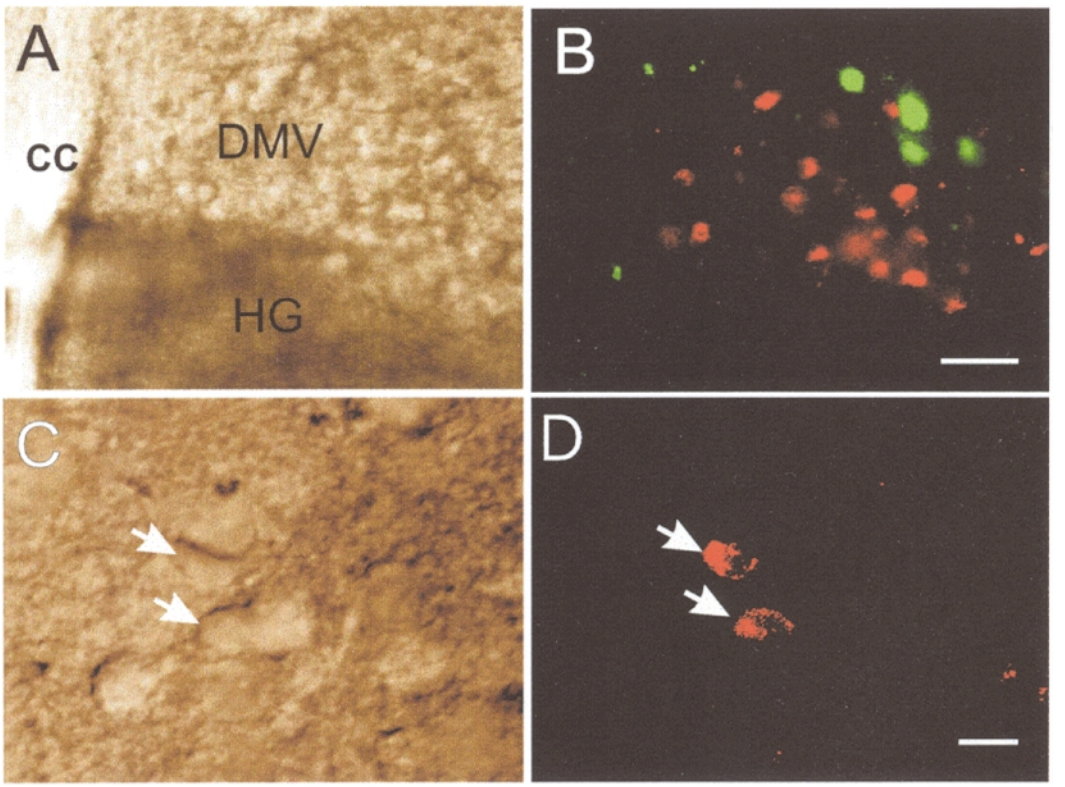

Figure 1. Identification of gastric-projecting DMV neurones in brainstem slices by retrograde labelling with DiI

A, brightfield photomicrograph at low magnification of a coronal slice through the caudal medulla at the level of the DVC. *B*, fluorescence photomicrograph of the same field of view as in *A*, illuminated through filters selective for TRITC (red) or FITC (green). Note the labelling of distinct groups of neurones following application of DiI to the gastric corpus (red) and application of DiO to the antrum/pylorus (green), respectively. Moreover, no instances were found in which DiI and DiO were co-localized in the same DMV neurone following apposition of these tracers to different regions of the GI tract in the same animal ($n = 13$). *C*, brightfield photomicrograph (DIC optics) at higher magnification of a region in medial DMV that contained neurones labelled with DiI but not DiO. Arrows indicate two corpus-projecting DMV neurones that were identified by the presence of DiI under fluorescence illumination. *D*, fluorescence (TRITC) photomicrograph of the same field of view as in *C* reveals the same two DiI-labelled neurones (marked by arrows). Scale bars represent 100 μm in panels *A* and *B*, 20 μm in panels *C* and *D*. Abbreviations: cc, central canal; DMV, dorsal motor nucleus of the vagus; HG, hypoglossal nucleus.

Table 1. Expression of responsiveness to orexin-A in subpopulations of DMV neurones that project to distinct regons of the GI tract

Group	Site of projection	Number tested	Number responsive	Percentage responsive	Group differences*
1	Fundus	22	15	68	3, 4, 5
2	Corpus	21	15	71	3, 4, 5
3	Antrum/pylorus	13	3	23	1, 2
4	Duodenum	18	4	19	1, 2
5	Caecum	13	1	8	1, 2
	Total	87	38	44	

* Significant difference compared to group shown ($P < 0.05$) by chi-square.

given DMV neurone (Fig. 2*B*, top and middle traces). However, the magnitude of the depolarization to a saturating concentration of peptide varied greatly between cells (8.1 ± 1.9 mV at 300 nM; 5 to 22 mV range, $n = 32$), and measurement of these responses was often obscured by the induction of firing. Therefore, evaluation of the concentration–response relationship for orexin-A-induced excitation was conducted in DMV neurones recorded under voltage clamp during pharmacological blockade of sodium-dependent spike activity (see below).

Administration of orexin-B (300 nM) produced depolarization and/or increased firing in a similar percentage of GI-projecting DMV neurones (48.6 %, 17 of 35), including 11 that also responded with excitation to orexin-A (Fig. 2*B*). The excitatory effects of orexin-B appeared indistinguishable from those of orexin-A and were observed over a similar range of concentrations (30–500 nM). Among 23 GI-projecting neurones that were tested with both peptides, 11 were excited by both orexin-A and orexin-B, 4 responded only to orexin-A, and 8 were unresponsive to either peptide.

DMV neurones respond to orexins in a viscerotopically organized manner

Earlier studies have shown that the majority of preganglionic motor neurones in the rat DMV are involved in regulating gastric function (Shapiro & Miselis, 1985), with the extent of vagal parasympathetic control over GI activity declining progressively as one proceeds distally from the duodenum into the colon (Berthoud *et al.* 1991). Given these considerations, we sought to determine whether responsiveness to orexins shows regional expression in preganglionic vagal motor neurones according to their site of projection in the GI tract. Table 1 summarizes the results from 87 recordings in which we compared the ability of orexin-A (300 nM) to excite DMV neurones labelled following placement of DiI to the gastric fundus ($n = 22$), corpus ($n = 21$), antrum/pylorus ($n = 13$), duodenum ($n = 18$) or caecum ($n = 13$). We found that responsiveness to orexin-A was preferentially expressed in gastric-projecting DMV neurones (69 % of fundus and corpus-projecting cells, $P < 0.05$) and rarely encountered in intestinal-projecting neurones, particularly among those providing innervation to more distal portions of the gut (cf. 19 % of duodenal-projecting *versus* only 8 % of caecum-projecting cells). Moreover, the responsiveness of gastric-projecting DMV neurones to orexin-A showed regional variations, with excitatory effects produced in a high percentage (70 %) of vagal motor neurones that innervate the fundus (15 of 22) or corpus (15 of 21), but in only 3 of 13 neurones identified as projecting to the antrum/pylorus (23 %, $P < 0.05$ compared to fundic or corpus neurones). On the other hand, the probability that a given neurone showed sensitivity to orexin-A bore no obvious relationship to its anatomical localization within the DMV. Thus, roughly 63 % of gastric-projecting neurones located in rostral DMV anterior of the area postrema (8 of 13) or in the caudal DMV, posterior to the obex (7 of 11), were excited by orexin-A (300 nM), compared to 74 % (15 of 19) of neurones examined that were localized to the intermediate portion of the nucleus (extending from the anterior border of the area postrema to the obex, as defined by Loewy (1990).

Mechanism of orexin-induced excitation

Additional kinds of experiments were performed to examine the cellular mechanism(s) responsible for the orexin-induced excitation in DMV neurones. For these experiments, corpus- or fundus-projecting neurones were targeted for study because of their high level and uniform pattern of responsiveness to orexin peptides. The depolarizing responses of DMV neurones to orexin-A ($n = 13$) or orexin-B ($n = 5$) were examined during blockade of synaptic transmission with tetrodotoxin (TTX) to determine whether the excitatory effects of the peptides were mediated directly, independent of an action on neighbouring neurones. Administration of TTX (2 μM) eliminated sodium-dependent spike activity in the slice as evidenced by blockade of current-evoked action potential firing. In 16 of 18 neurones examined, the depolarizing responses to orexin-A or orexin-B continued unabated in the presence of TTX (Fig. 2*B*), suggesting they resulted from the activation of postsynaptic receptors and were not dependent on impulse-dependent synaptic transmission. Under these conditions, a small, but significant increase in membrane resistance (112 ± 0.9 %, range 107–120 %,

$n = 11$, $P < 0.05$) was seen to accompany the depolarizing response to either form of orexin, indicating further that the peptides increase excitability in DMV neurones in part by decreasing an outward ionic conductance. Moreover, in all but two of the neurones, administration of orexins in the presence of TTX induced the repetitive firing of spontaneous, low amplitude spike discharges (Figs 2*B* and 3). These TTX-insensitive spike discharges were abolished by bath superfusion of the non-selective Ca^{2+} channel blocker Cd^{2+} (300 μM; 3 of 3 neurones tested), and therefore most likely represented calcium spikes mediated via influx of Ca^{2+} through voltage-gated Ca^{2+} channels (Fig. 3). On the other hand, perfusion of the slice with Cd^{2+} had no significant effect on the amplitude or duration of the orexin-induced depolarization. The latter result argues against the likelihood that the orexin-induced depolarization resulted from changes in Ca^{2+} conductance, while providing additional evidence that these responses were mediated directly via activation of postsynaptic orexin receptors.

To further characterize the conductance(s) responsible for the depolarizing effect of orexin-A, DMV neurones were recorded in voltage-clamp mode at 34 °C. In the first series of experiments, neurones ($n = 17$) were held at −60 mV in Krebs solution containing TTX (2 μM) and orexin-A administered over a threefold range of concentrations (10–1000 nM) in randomized order, to determine the concentration–response relationship for peptide-induced changes in holding current. Administration of orexin-A at or in excess of 30 nM induced a slowly developing inward current, whose peak amplitude at maximal concentrations of peptide averaged −72 ± 11 pA (42 to 132 pA range, $n = 11$) (Fig. 4). The graph in Fig. 4*B* shows the concentration–response relationship for the orexin-A-induced inward current, generated by pooling results from three to six neurones, tested with at least three concentrations of peptide. The concentration–response relationship for the orexin-A-induced inward current was relatively narrow with a threshold concentration of 30 nM,

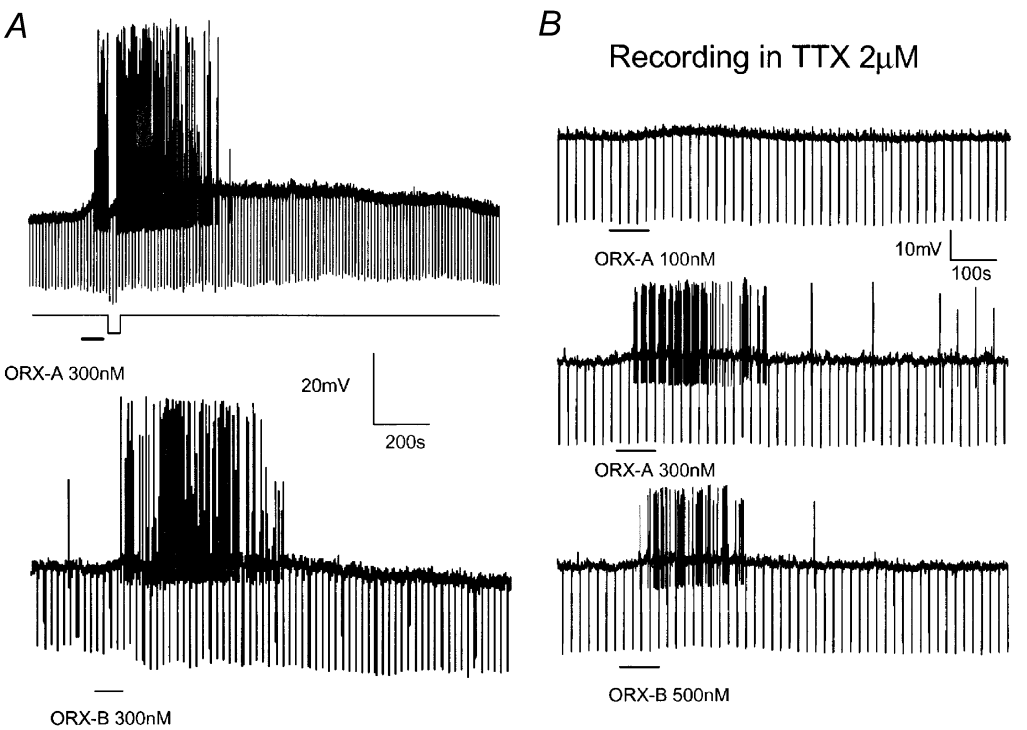

Figure 2. Orexins directly depolarize DMV neurones and increase spike firing

A, perfusion of orexin-A (top trace) or orexin-B (lower trace) produced depolarization, accompanied by an increase in spontaneous firing, in two different gastric-projecting DMV neurones. Downward deflections in the traces are electrotonic potentials induced by passage of hyperpolarizing constant current pulses through the recording electrode that were used to measure membrane input resistance. Note that the amplitudes of the electrotonic potentials were increased during the orexin-induced depolarizations, indicating that the peptides increased membrane input resistance. The current monitor directly below the trace of membrane voltage (in *A*) illustrates the time during the orexin-induced depolarization that the membrane potential was returned to the resting level by passage of hyperpolarizing current. *B*, recordings from a single DMV neurone obtained during perfusion of the slice with TTX (2 μM) to block impulse-dependent synaptic transmission. Administration of orexin-A or orexin-B produced concentration-dependent membrane depolarization via a postsynaptic action. Both peptides also promoted the occurrence of spontaneous low amplitude spike discharges that were TTX insensitive. The holding potential was −60 mV (top) and −62 mV (bottom) for the neurones in *A*, and −60 mV for the neurone in *B*.

estimated EC_{50} of 100 nM and maximal response produced at 300 nM of the peptide.

In a subsequent series of experiments ($n = 6$), we examined the reversal potential for the orexin-induced inward current. Steady state current–voltage (*I–V*) relationships were determined for each neurone in normal Krebs solution containing TTX (2 μM) and during superfusion of similar media containing orexin-A (300 nM), and the corresponding pairs of currents recorded at each potential were subtracted to reveal the *I–V* relationship for the peptide-induced inward current (Fig. 5*A*). The slope conductance of steady-state *I–V* curves measured between −100 and −50 mV was decreased by orexin-A (2.8 ± 0.3 *vs.* 3.2 ± 0.5 nS, $P < 0.05$) in 5 of 6 neurones. In these cells, the *I–V* relationship for the orexin-induced current was essentially linear over the same range of potentials, as shown for example by the results from a representative experiment depicted in Fig. 5*B*. In addition, the extrapolated reversal potential of the orexin-induced inward current was −99 ± 2.4 mV, which was close to that predicted for a pure K^+ conductance (−107 mV) under our recording conditions ($[K^+]_{ext}$ = 2.5 mM, 34° C). In the remaining neurone, the steady state *I–V* curve for the orexin-induced current showed a parallel shift and did not reverse polarity over the entire voltage range examined. Currents of this type have been described previously in DMV neurones (Hwang *et al.* 2001) and were attributed to a combined action of orexin involving inhibition of a resting K^+ conductance and activation of non-selective cation channels. It was also suggested that this is the primary mechanism by which orexins directly excite DMV neurones in the rat, although this conclusion was based on sampling from an undefined population of cells (Hwang *et al.* 2001).

The results from the studies above are more consistent with a reduction in K^+ conductance as the primary basis for the orexin-induced postsynaptic excitation in gastric-projecting DMV neurones. To test this hypothesis, additional types of experiments were conducted under voltage clamp in a separate group of corpus-projecting DMV neurones ($n = 28$) and responses measured to a single application of orexin-A (300 nM). In the first series, depolarizing voltage ramps (20 mV s^{-1}) were used to determine the steady-state *I–V* relationship for the orexin-A-induced inward current over an extended range of membrane potentials (−140 to −40 mV) and the current was examined for reversal in its polarity. In 8 of 11 recordings obtained in normal Krebs solution, the orexin *I–V* curve was essentially linear between −60 and −125 mV, and in these neurones the orexin-A-induced inward current reversed at membrane potentials (106 ± 3.2 mV) nearly identical to E_K (Fig. 6*A*). In the three remaining neurones,

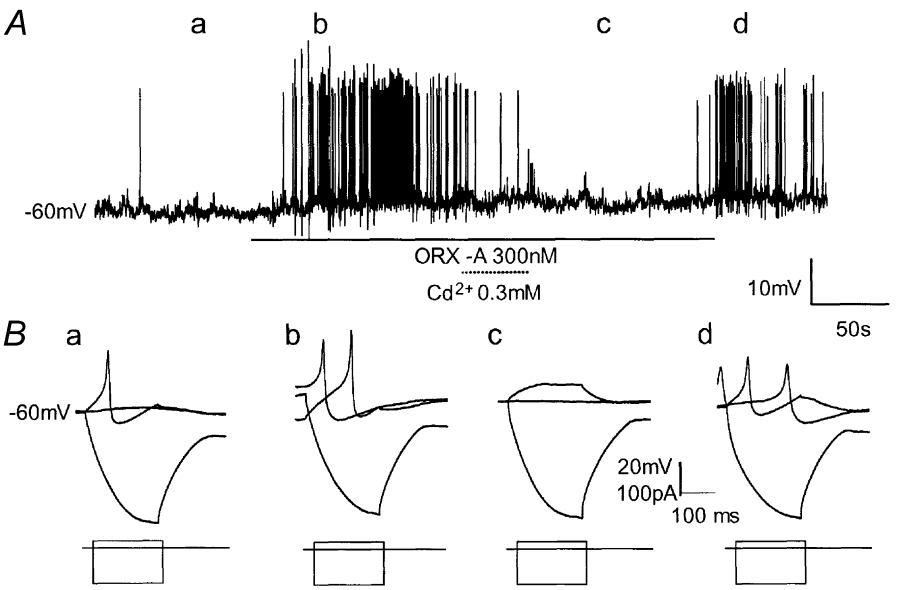

Figure 3. Orexin-A promotes Ca^{2+}-dependent spike discharge in DMV neurones

A, administration of orexin-A (300 nM) in the presence of TTX evoked a prolonged discharge of low amplitude spikes, which occurred despite little change in resting membrane potential. This TTX-insensitive spike activity was reversibly eliminated by administration of the non-selective Ca^{2+} channel blocker, Cd^{2+} (300 μM), indicating it consisted of Ca^{2+}-dependent action potentials. The neurone was current-clamped at −60 mV holding potential. *B*, family of membrane responses (upper traces) to passage of constant current hyperpolarizing (−0.1 nA) and depolarizing (+0.02 nA) pulses (lower traces) through the recording electrode at the times and under the conditions indicated (corresponding to letters *a–d*) in the voltage trace (*A*). Orexin-A promoted the discharge of Ca^{2+}-dependent action potentials at resting and depolarized levels of membrane potential, and this effect was blocked reversibly by Cd^{2+}.

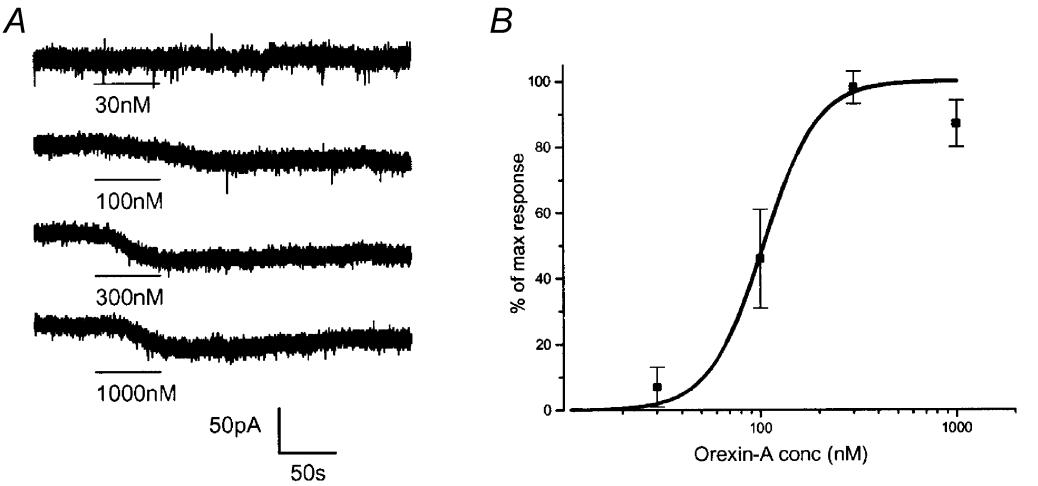

Figure 4. Concentration–response relationship for orexin-A-induced inward current

A, family of current traces recorded in a DMV neurone voltage-clamped at −60 mV holding potential in response to administration of increasing concentrations of orexin-A. *B*, concentration–response relationship for inward shift in holding current produced by orexin-A (10–1000 nM). Each point (filled squares) represents the mean ± S.E.M. (capped bars) of the normalized orexin-induced inward current, generated by pooling results from 3–6 neurones, tested with at least three concentrations of peptide. The line was fitted to the data points using the Hill equation: $I/I_{max} = C^n/(C^n + EC_{50}{}^n)$, where I is the measured current at drug concentration C; EC_{50} is the concentration of drug producing a 50 % response, and n is the Hill coefficient.

orexin-A induced an inward current that decreased with hyperpolarization (between −40 and −90 mV), but did not reverse in the entire voltage range examined (Fig. 6*B*).

To further evaluate the involvement of K^+ conductance, steady state *I–V* curves for orexin-A-induced currents were measured in a high-K^+ (15 mM) Krebs solution in five additional neurones. We noted in our earlier studies that the response to orexin-A typically declined with each successive application of peptide (but see the neurone depicted in Fig. 5). To prevent this from biasing the results, the effect of orexin-A on membrane current was

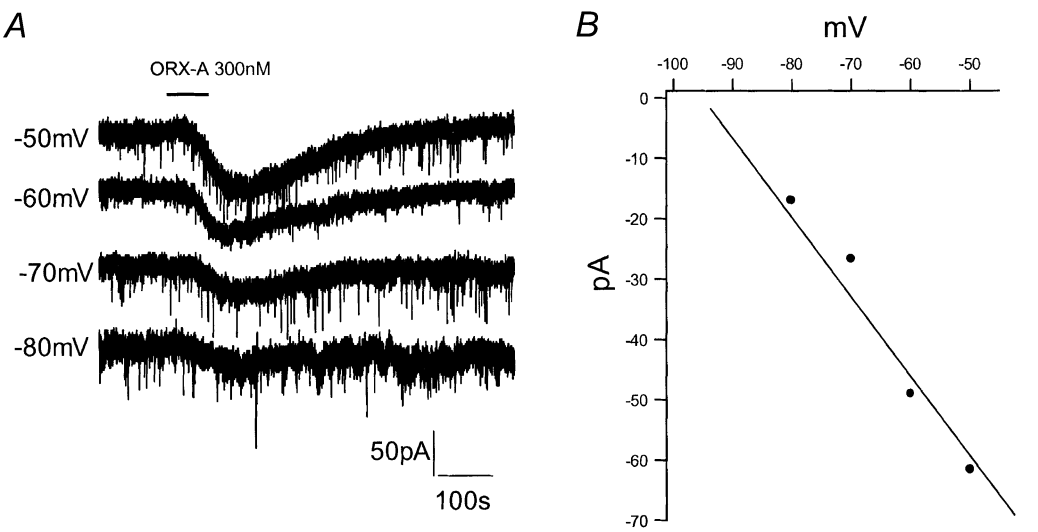

Figure 5. *I–V* relationship for the orexin-induced inward current in DMV neurones

Traces in *A* illustrate the change in orexin-A-induced inward current recorded in a gastric-projecting DMV neurone as a function of the holding potential. Note the progressive decrease in magnitude of the orexin-induced inward current with membrane hyperpolarization. *B*, *I–V* relationship for the inward current responses for the neurone depicted in *A*, generated by plotting the peak amplitude of the peptide-induced current as a function of the holding potential. In this neurone the *I–V* relationship was essentially linear over the voltage range of −50 to −90 mV and yielded an estimated reversal potential of −96 mV for the peptide-induced inward current. These experiments were performed in the presence of TTX (2 μM).

determined in high-extracellular [K^+], without prior testing in normal Krebs solution, and neurones were included for analysis if the orexin-induced current showed a clear reversal potential. In four of five neurones tested, the *I–V* curves revealed orexin-induced currents that reversed between −65 and −58 mV (Fig. 6*C*), with the reversal potential shifting to −62 ± 6 mV in 15 mM extracellular K^+, which is close to the value predicted for a pure K^+ conductance under these conditions (−60.2 mV at 34° C). We also examined for dependence of the orexin-induced inward current on K^+ conductance by recording from DMV neurones using patch pipettes filled with CsCl

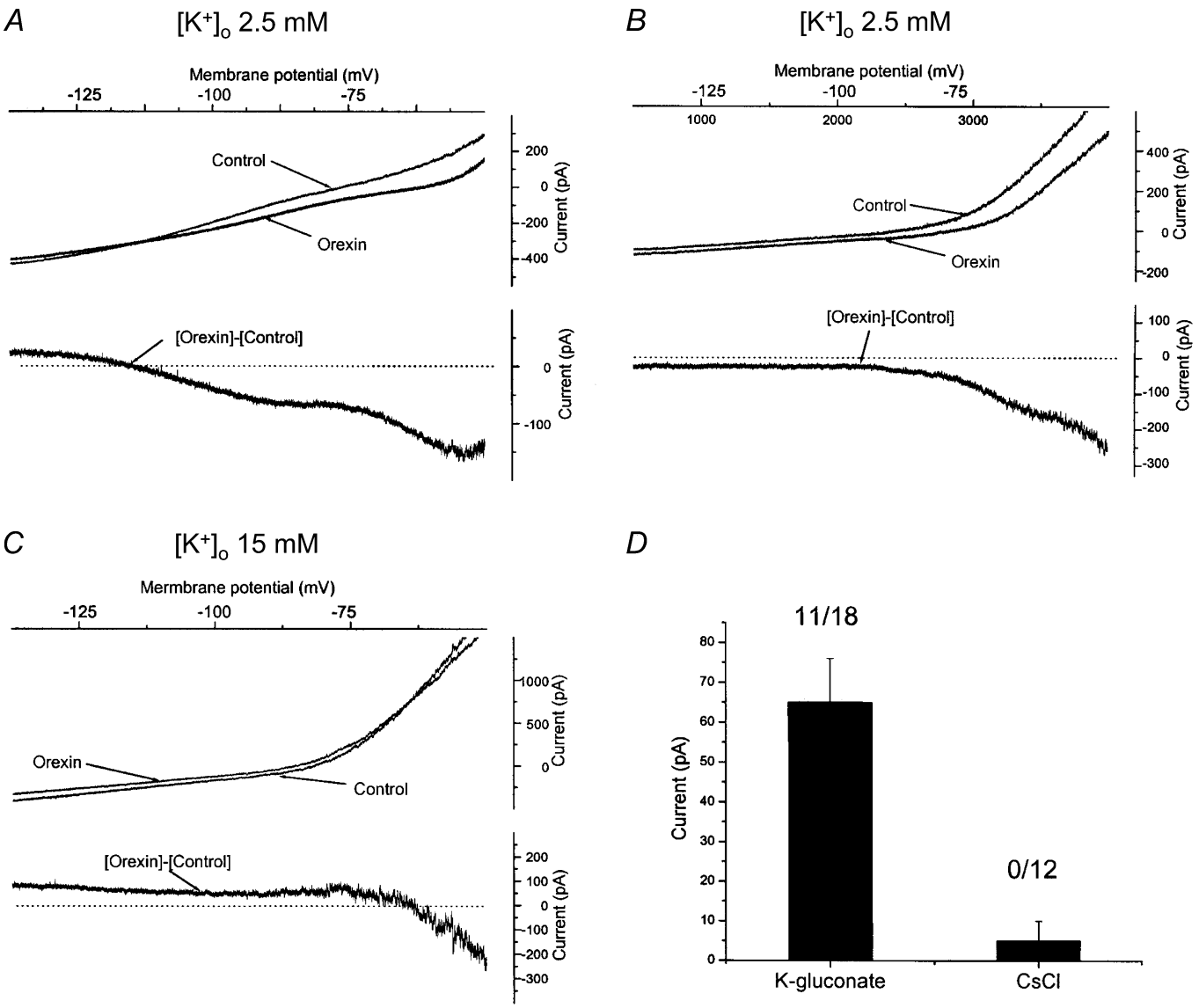

Figure 6. Decrease in K^+ conductance largely accounts for orexin-induced inward current in gastric-projecting DMV neurones

A, superimposition of *I–V* relationships generated to a voltage ramp from −140 mV to −40 mV in normal Krebs (control) and during administration of orexin (300 nM). Administration of orexin to this neurone decreased whole-cell slope conductance and induced a linear inward current over the range of −125 to −60 mV. A subtraction trace (lower panel) shows the orexin-induced current reversed near E_K (approx. −107 mV) (lower panel). *B*, *I–V* curves from a different corpus-projecting DMV neurone in which orexin-A induced a small inward current that did not reverse over the entire voltage range tested (lower panel). *C*, *I–V* relationship for the orexin-induced current response of another DMV neurone determined during perfusion of high-K^+ (15 mM)-containing Krebs solution. In this neurone, the orexin-induced current was accompanied by little change in slope conductance over an extended range of membrane potentials, yet reversed near to E_K (−60 mV) as predicted for these recording conditions. *D*, average amplitude of orexin-A-induced inward current (measured at −60 mV holding potential) for DMV corpus-projecting DMV neurones recorded with patch pipettes filled with potassium gluconate (n = 18) or CsCl (n = 12). The number of neurones that responded to the peptide with an inward current under each condition is indicated above the bar.

(145 mM), which blocks a variety of K^+ channels. Under these conditions, administration of orexin did not produce a significant change in membrane current in any of the 12 neurones examined (Fig. 6*D*). Taken together, these data suggest that orexin-A produces direct excitation in a majority of gastric-projecting DMV neurones via a Cs^+-sensitive mechanism, involving reduction of a K^+ current.

Effect of orexins on synaptic currents in DMV neurones

Orexins have been shown to modulate synaptically evoked activity in a variety of target neurones, resulting in actions that can reinforce as well as oppose the direct excitatory effects of the peptides on neuronal excitability (van den Pol *et al.* 1998; Kirchgessner & Liu, 1999; Liu *et al.* 2002). To examine for a presynaptic action of the peptide on afferent input to DMV neurones, pairs of excitatory or inhibitory postsynaptic currents (EPSCs and IPSCs) were evoked by repetitive electrical stimulation in NTS and the averaged responses to 10 stimulation trials compared before, during and after washout of orexin-A (300 nM) from the bath. Electrical stimulation delivered to the NTS subnucleus medialis or commissuralis evoked inwardly directed EPSCs, outward IPSCs, or biphasic EPSC–IPSC responses in 38 of 51 DMV neurones, recorded at −60 mV holding potential. The inward synaptic currents were reduced in amplitude and duration by administration of APV (50 μM) and blocked completely by addition of CNQX (20 μM) alone (6 of 11 neurones) or when applied in combination with APV (Fig. 7*A*, remaining five neurones). These results are congruent with earlier reports that document the involvement of both NMDA-type and AMPA-type glutamate receptors in the generation of EPSCs in rat DMV neurones (Willis *et al.* 1996; Bertolino *et al.* 1997; Browning *et al.* 2002). Conversely, the outward components of all postsynaptic currents (PSCs) were blocked by bath application of picrotoxin (4/4 neurones) or BMI (30 μM) (10 of 10 neurones, Fig. 7*B*), consistent with previous studies that indicate mediation of these inhibitory responses via release of GABA and activation of postsynaptic $GABA_A$ receptors (Travagli *et al.* 1991; Bertolino *et al.* 1997; Browning & Travagli, 1999). Additionally, we found that administration of BMI increased the amplitude of evoked EPSCs in 5 of 7 neurones examined (Fig. 7*C*), suggesting that focal electrical stimulation to a localized site within the NTS might activate both inhibitory and excitatory inputs that converge onto a single DMV neurone.

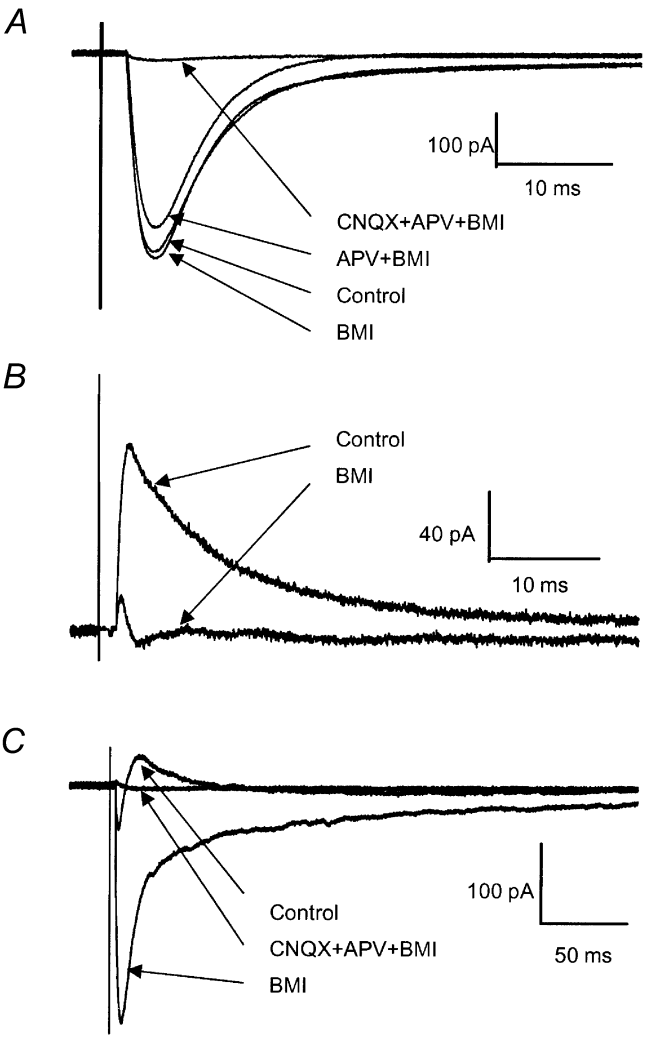

Figure 7. Pharmacological dissection of glutamatergic EPSCs and GABAergic IPSCs evoked in DMV neurones in response to electrical stimulation in NTS subnucleus commisuralis or medialis

The traces in panels *A*–*C* represent synaptic currents evoked in three different gastric-projecting DMV neurones. *A*, the amplitude of the NTS-evoked EPSC was slightly enhanced during perfusion of BMI (30 μM), whereas it was reduced by administration of APV, a selective NMDA-type glutamate receptor blocker. Administration of APV (50 μM) in combination with CNQX (20 μM), an AMPA-type glutamate receptor blocker, completely abolished the EPSC. *B*, the NTS-evoked IPSC recorded in another neurone was largely eliminated during superfusion of BMI (30 μM), a selective $GABA_A$ receptor antagonist. *C*, stimulation in NTS subnucleus medialis evoked synaptic currents in a third neurone that were sensitive to BMI and glutamate receptor antagonists. In this neurone, blockade of an IPSC following administration of BMI unmasked a small EPSC that was eliminated by the combined application of APV and CNQX. Holding potential was −60 mV for the neurones in *A*–*C*.

The effects of administration of orexin-A or orexin-B (300 nM) were examined on stimulation-evoked excitatory or inhibitory currents in 31 GI-related DMV neurones, of which 17 projected to the gastric fundus or corpus, 4 to the antrum/pylorus, 7 to the duodenum, and 3 innervated the caecum. Superfusion of orexin-A or orexin-B had no significant effect on the peak amplitude of the NTS-evoked EPSCs in any neurones ($n = 9$), regardless of their site of projection in the GI tract (95 ± 3.9 % of control, $P = 0.35$). On the other hand, the peak amplitude of NTS-evoked IPSCs was reversibly increased by administration of either orexin-A or orexin-B in 5 of 22 neurones tested (115 ± 6.1 %, $P < 0.05$, Fig. 8*A*). In addition, in three of the five neurones administration of orexin-A unmasked outward currents that showed sensitivity to blockade by TTX (2 μM) and by the selective $GABA_A$ receptor antagonist BMI (30 μM) (Fig. 8*B*). Interestingly, all five neurones were identified as projecting either to the fundus or corpus; however, none of them showed excitation or a depolarizing shift in holding current (when clamped at −60 mV holding potential) in response to application of the peptide.

The results from the latter experiments suggest that orexins may act indirectly to modulate excitability in a small subset of gastric-projecting DMV neurones by facilitating the evoked release of GABA from NTS neurones. In an initial test of this hypothesis, we next examined whether the enhancement of NTS-evoked IPSCs by orexin-A was associated with a change in the paired-pulse ratio. The ratio of the amplitude of two postsynaptic currents evoked a few milliseconds apart has been used routinely to determine the pre- *versus* postsynaptic site of drug action (Trombley & Westbrook, 1992; Travagli & Williams, 1996), with a change in the ratio being taken as an indication of a presynaptic effect. Figure 9 illustrates the results from a representative experiment conducted in DMV neurones that showed peptide-induced enhancement of the NTS-evoked IPSC. When two IPSCs were evoked 100 ms apart in this DMV neurone, the second IPSC (S_2) was smaller than the first (S_1). In the presence of orexin-A (300 nM) the paired-pulse ratio (S_2/S_1) increased from 0.64 in control to 0.78 (Fig. 9*C*), suggesting that the enhancement of the evoked IPSC resulted from actions of the peptide at a presynaptic site. Results from four neurones examined in this manner revealed that the paired-pulse ratio obtained from averaging all of the traces in the presence of orexin-A was larger than the corresponding ratio obtained from traces generated under control conditions (0.83 ± 0.8 *vs.* 0.58 ± 0.7, $P < 0.05$).

Next, we examined for an effect of orexin-A on spontaneous IPSCs (sIPSCs) to determine whether the facilitation of inhibitory input onto DMV neurones arose indirectly from excitation of GABAergic NTS neurones or resulted from actions of the peptide on NTS nerve terminals. In these experiments, recordings were obtained from corpus-projecting DMV neurones using KCl-filled pipettes and CNQX (20 μM) and APV (50 μM) included in the bath solution to eliminate contamination by EPSCs (see Methods). Using KCl-filled pipettes shifted the reversal potential for Cl^- to near 0 mV, such that sIPSCs appeared as inward currents and were more readily detected (compared with potassium gluconate recordings), being of larger amplitude at the holding potential

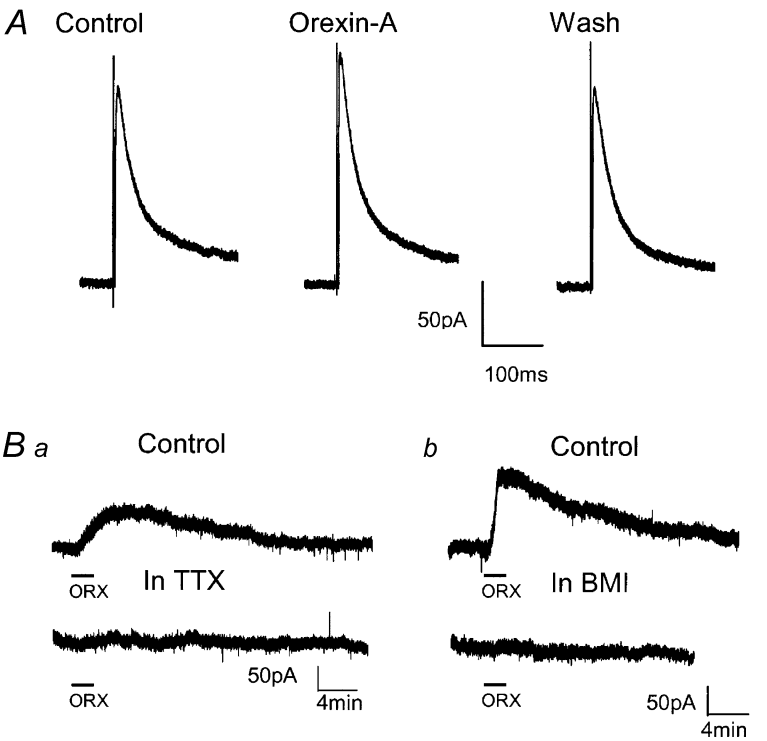

Figure 8. Orexin-A enhances synaptic inhibition in a subset of DMV neurones

A, administration of orexin-A enhanced the amplitude of IPSCs evoked by electrical stimulation in NTS subnucleus commisuralis. Responses were recorded at −60 mV holding potential. *B*, current traces recorded in two different neurones illustrate the unmasking of a tonic inhibitory outward current following administration of orexin-A (300 nM). In the neurone depicted in *Ba*, administration of orexin-A (bar) induced a prolonged outward current that was sensitive to blockade by TTX (2 μM) (lower trace). In a second neurone (*Bb*), the orexin-induced outward current was blocked entirely by administration of the selective $GABA_A$ receptor antagonist, BMI. Neurones depicted in *B* were voltage-clamped at a holding potential of −60 mV.

(−60 mV). The frequency of sIPSCs was reversibly increased by orexin-A (300 nM) in 4 of 20 neurones tested (Fig. 10), which is in keeping with the low incidence of neurones showing enhancement in stimulation-evoked inhibition, as described above. In these four neurones, orexin-A increased the frequency of sIPSCs by 73–345 % and also enhanced the mean amplitude of the synaptic current (from 45 ± 7 pA to 79 ± 6 pA, $P < 0.01$) (Fig. 10*B*). No effect of orexin-A on sIPSC frequency or amplitude was observed in the remaining 16 neurones.

Finally, to determine if the increase in IPSC frequency induced by orexin-A was due to stimulation of NTS neurone activity, the peptide was applied during blockade of impulse-dependent release with TTX in five cells, including three in which sIPSC frequency was increased by orexin-A in normal Krebs solution. As shown in Fig. 10*C*, the frequency of mIPSCs was not affected by administration of orexin-A in any of these corpus-projecting DMV neurones ($P > 0.05$). In all cases, these spontaneous inward currents were blocked by BMI (30 μM), indicating that they were mIPSCs (Fig. 10*C*).

DMV neurones show differential responsiveness to orexins and OT

Electrophysiological recordings obtained from DMV neurones *in vivo* and in brainstem slice preparations demonstrate that a large percentage of preganglionic vagal motor neurones are endowed with functional OT receptors, whose activation causes an increase in neuronal excitability (McCann & Rogers, 1990; Dubois-Dauphin *et al.* 1992; Raggenbass & Dreifuss, 1992). Others have shown that microinjection of OT into the DMV in anaesthetized rats increases the excitability of neurones that receive excitatory drive from gastric vagal mechanoreceptors, thereby potentiating vago-vagal reflexes that modulate gastric motility and secretion (Rogers & Hermann, 1987; McCann & Rogers, 1990). On the other hand, blockade of central OT receptors has been reported to increase baseline gastric motility in adult rats (Flanagan *et al.* 1992), suggesting that endogenous OT may exert tonic inhibitory control over specific components of vagal efferent outflow and thus counterbalance the stimulatory effects of orexins on gastric motor function. Presuming this model to be true, we hypothesized that OT and orexins may act either selectively or in a differential manner to modulate the excitability of distinct populations of gastric-projecting DMV neurones. To test this hypothesis, we compared the ability of orexin-A and OT to produce excitation in the same DMV neurones, using membrane depolarization and/or increase in firing as an index of postsynaptic responsiveness, and correlated the sensitivity of individual vagal neurones to each peptide with their site of projection in the GI tract. The effects of bath administration of OT in saturating concentrations (typically 300 nM) were examined in current-clamp recordings from 40 GI-projecting DMV neurones that were also tested for responsiveness to orexin-A (300 nM). Slightly less than half (18 of 40) of the DMV neurones responded to OT, with the typical response consisting of a slow depolarization and/or increase in spontaneous firing, associated with little change or a small increase in membrane conductance (Fig. 11*A*). The excitatory responses to OT appeared remarkably similar to those produced by orexin-A in terms of their amplitude and prolonged time course. However, only a few DMV neurones were encountered that responded with excitation to both peptides. Table 2 summarizes the results

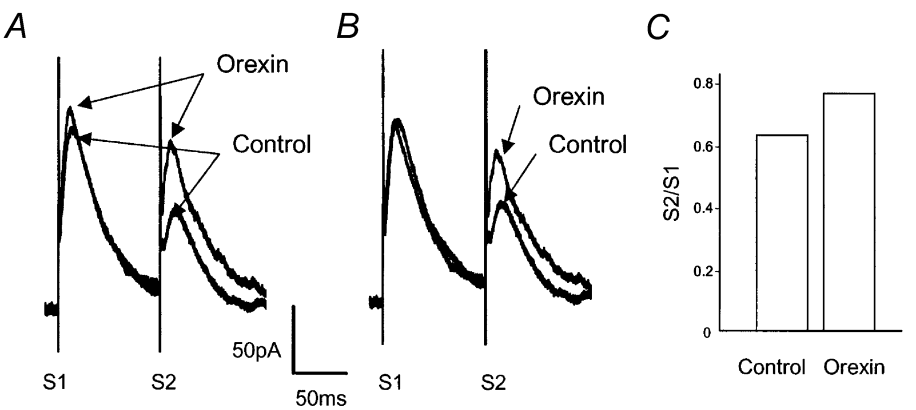

Figure 9. Enhancement of the IPSC by orexin-A is accompanied by a change in the paired-pulse ratio

A, representative traces showing pairs of IPSCs evoked 100 ms apart before and during administration of orexin-A (300 nM). Orexin-A increased the amplitude of the NTS-evoked inhibitory currents. *B*, the alteration of the paired-pulse ratio (S_2/S_1) for the traces depicted in *A* is easily seen after normalizing to control (pre-drug) amplitude the amplitude of the IPSC evoked by the first pulse (S_1). Traces are the average of 10 trials each. Holding potential was −60 mV. *C*, the paired-pulse ratio compares the amplitude of the second current (S_2) with that of the first current response (S_1), which in this neurone was increased from 0.64 in control to 0.78 in the presence of orexin-A.

from 40 experiments in which excitatory responsiveness to OT and orexin-A was compared in the same DMV neurones, categorized according to their site of GI projection. Two major findings are apparent from these data: first, only 6 of 18 neurones that were excited by OT were also responsive to orexin-A, and most of these (4 of 6) innervated the gastric fundus. Second, in contrast to what was found with orexins (see Table 2), responsiveness to OT was uniformly expressed among DMV neurones that project to the different regions of the stomach or to the duodenum. From these experiments we conclude that orexin-A and OT exert their respective influence on specific components of vagally dependent GI functions primarily by modulating excitability of distinct groups of GI-projecting vagal neurones, rather than through differential actions exerted on a common pool of vagal motor neurones.

DISCUSSION

The present study demonstrates that the hypothalamic peptides orexin-A and orexin-B have excitatory effects in many DMV neurones in the rat, including a large

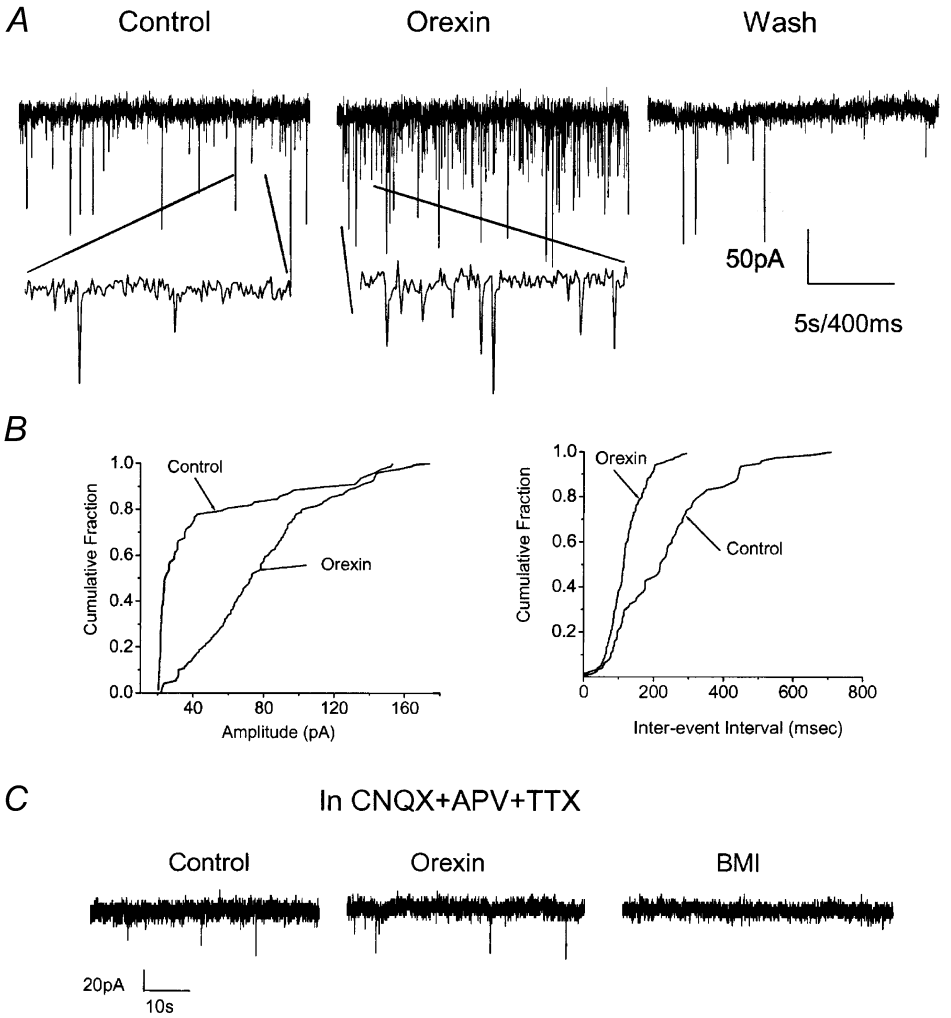

Figure 10. Effect of Orexin-A on inhibitory synaptic input

A, current traces recorded from a voltage-clamped corpus-projecting DMV neurone show an increase in spontaneous IPSCs induced by administration of orexin-A (300 nM). Holding potential was −60 mV. The lower records correspond to the areas designated in the upper traces, depicted at expanded time scale. Recordings were obtained in the presence of APV (50 μM) and CNQX (20 μM) to eliminate EPSCs and using KCl-filled electrodes, such that Cl^--mediated IPSCs appear as inward currents. The stimulatory effect of orexin-A on IPSC frequency was reversible, with recovery of PSC frequency to the control level following 40 min washout of peptide from the bath. *B*, cumulative distributions of PSC amplitude (left) and inter-event intervals (right) for the same cell before and during the application of orexin-A indicate that the peptide increased the amplitude ($P < 0.05$) and frequency of sIPSCs ($P < 0.05$). *C*, traces from another corpus-projecting DMV neurone recorded in the presence of TTX (2 μM) reveal no effect of orexin-A (300 nM) on the frequency of mIPSCs. The occurrence of mIPSCs was abolished by administration of the $GABA_A$ receptor blocker BMI (30 μM). Holding potential was −60 mV.

Table 2. Comparison of responsiveness to oxytocin (OT) and orexin-A in DMV neurones that project to different parts of the GI tract

Site of projection	No. tested	No. OT responsive	No. orexin-A responsive	No. OT and orexin-A responsive
Fundus	14	7	8	4
Corpus	5	3	3	1
Antrum/pylorus	8	4	2	0
Duodenum	6	4	2	1
Caecum	7	0	1	0
Total*	40	18	16	6

*Values indicate the total number of DMV neurones of designated GI projection among 40 tested that responded with excitation to OT alone, orexin-A alone, or to both peptides.

percentage of preganglionic vagal motor neurones that innervate the upper GI tract. The excitatory effects of orexin peptides were manifested by a prolonged membrane depolarization, accompanied by an increased frequency of action potential discharge. The depolarizing responses to orexins persisted in the presence of TTX and during blockade of Ca^{2+}-dependent synaptic activity with Cd^{2+}, indicating that they resulted from a direct action of the peptides on the recorded neurone, rather than via interactions at a presynaptic site. In addition, orexins induced a barrage of low amplitude spike discharges that were unaffected by TTX, but were eliminated in a reversible manner by administration of Cd^{2+}. The latter results indicate that these peptides promote Ca^{2+}-dependent spike firing in DMV neurones, presumably via enhancement of Ca^{2+} influx through voltage-dependent Ca^{2+} channels, similar to the effects found in locus coeruleus neurones (Horvath *et al.* 1999*b*) and in hypothalamic neuronal cultures (van den Pol *et al.* 1998). Adding support to this are results from preliminary studies that demonstrate the ability of orexin-A to modulate specific components of depolarization-evoked whole-cell Ca^{2+} current in acutely dissociated DMV neurones (Zhou *et al.* 2001).

Hwang *et al.* (2001) reported in a recent study that orexin-A and orexin-B produced postsynaptic depolarization and increased firing in approximately 30% of rat DMV neurones examined at random. They also showed that the vast majority of DMV neurones that responded with

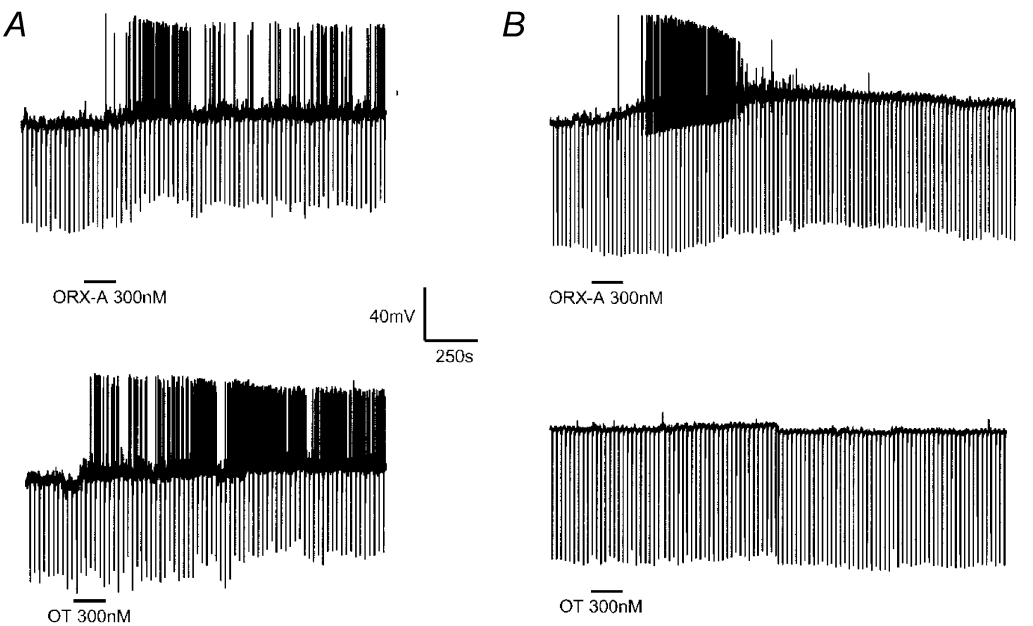

Figure 11. Comparative effects of OT and orexin-A in the same DMV neurone

Traces from current-clamp recordings in *A* and *B* illustrate the responses of two DMV neurones to sequential administration of orexin-A (300 nM) and OT (300 nM). *A*, brief application of either peptide produced prolonged depolarization and increased spike firing in a fundus-projecting vagal motor neurone. *B*, by contrast, a corpus-projecting DMV neurone was excited by orexin-A, but showed no response to administration of a high concentration of OT. The holding potential was −60 mV for both neurones.

excitation to orexins represented preganglionic parasympathetic motor neurones, as determined by their retrograde labelling following intraperitoneal injection of Fluorogold (Powley *et al.* 1987). Our results are consistent with the observations of these investigators and extend them in a number of ways. First, we demonstrated that preganglionic vagal motor neurones respond to orexin peptides in a viscerotopic manner according to the specific site of a neurone's projection in the GI tract. Thus, a large majority of vagal motor neurones that project to the gastric fundus or corpus (~70 % of those tested) responded to orexin-A or orexin-B with depolarization and increased action potential firing. In contrast, responsiveness to either form of peptide was observed in a much smaller percentage of DMV neurones that supplied the gastric antrum/pylorus (23 %) or duodenum (~19 %) and rarely encountered in vagal neurones that innervated the caecum (~8 %). Second, we obtained evidence that orexin-A evokes depolarization in gastric-projecting vagal motor neurones primarily by decreasing a resting K^+ conductance. In addition, we found that in a subset of these neurones, orexin-A modulates membrane excitability indirectly by acting presynaptically to enhance GABA-mediated synaptic input from the NTS. Lastly, we showed that orexins and OT produce similar excitatory effects in many GI-projecting vagal motor neurones, but that responsiveness to OT is uniformly expressed among DMV neurones that project to different regions of the GI tract. Moreover, direct comparison of the effects of orexin and OT in the same neurone revealed that for the most part these peptides influence distinct populations of preganglionic vagal motor neurones. Each of these findings is considered in greater detail below and their functional significance discussed.

Responsiveness to orexins is viscerotopically organized

Results from recent immunohistochemical studies indicate that the majority of DMV neurones in the rat express orexin receptors, with the orexin-1 receptors (OR1) found in greater abundance than orexin-2 receptors (OR2) (Krowicki *et al.* 2002). In addition, Krowicki *et al.* (2002) showed by combining immunostaining for OR1 with retrograde labelling of neurones following injections of fluorescently tagged cholera toxin into the gastric wall that OR1 is expressed in a majority of preganglionic vagal motor neurones that innervate the stomach. The finding in the present study that roughly 70 % of fundus- and corpus-projecting DMV neurones were excited by orexin peptides is consistent with these anatomical data. Our results suggest further that relatively few vagal neurones that supply the gastric antrum/pylorus express receptors for orexins on their cell bodies. Marcus *et al.* (2001) demonstrated using *in situ* hybridization histochemistry that OR1 and OR2 have distinct expression patterns throughout the rat brain, and thus it is conceivable that these two receptor types may be expressed differentially in DMV neurones that project to distinct regions of the GI tract. However, this could not account for the low incidence of electrophysiological responses to orexin-A found in antrum/pylorus-projecting DMV neurones, given that both receptor types have been shown to exhibit equally high functional affinity for this peptide (Sakurai *et al.* 1998; Smart *et al.* 1999). Currently, we are examining the effects of microinjection of orexins into the DMV on regionally specific measurements of gastric contractility to determine whether the centrally mediated actions of these peptides evoke changes in gastric motility and/or tone in proximal, but not distal portions of the stomach, as predicted by the results from our electrophysiological experiments.

In contrast to vagal motor neurones that send projections to the gastric fundus or to the corpus, those that supplied the small intestine or more distal colon were typically unresponsive to orexin peptides. This differential pattern of DMV neurone responsiveness to orexins largely coincides with the topography of vagal efferent innervation of the rat GI tract. Thus, the vast majority of preganglionic parasympathetic vagal neurones have been shown to heavily innervate the stomach and most proximal portions of the duodenum, while providing sparse projections to distal portions of the intestine and the colon (Berthoud *et al.* 1991). Similarly, the finding that orexins directly excite a high percentage of fundus- and corpus-projecting DMV neurones provides a cellular basis for the stimulation of gastric acid secretion and contractile activity produced following intracerebroventicular administration (Takahashi *et al.* 1999) and microinjection of orexin-A into the DMV (Krowicki *et al.* 2002), respectively. Interestingly, the pattern of response to orexins exhibited among different groups of GI-projecting vagal neurones contrasts with the organizational scheme encountered in the enteric nervous system, where the distribution of orexin-containing neurones, nerve fibres and orexin receptors suggests that the physiological actions of this intrinsic peptidergic innervation are preferentially concentrated on lower portions of the GI tract (Kirchgessner & Liu, 1999; Naslund *et al.* 2002), Congruent with this, Kirchgessner & Liu (1999) reported that superfusion of orexin-A stimulates motility in isolated guinea-pig distal colon. In addition, it was recently shown in rat that intravenous infusion of orexin-A or orexin-B inhibits the myoelectric motor complex in the small intestine, mediated through a peripheral action of the peptides exerted presumably on enteric neurotransmission (Naslund *et al.* 2002). Taken together, these results provide evidence for a functional partitioning of the GI effects produced by central release of orexins from hypothalamic projections into the DMV and those mediated peripherally by the intrinsic orexin

innervation of the gut. Earlier findings in the rat that intracisternal administration of orexin-A stimulates gastric acid secretion via a vagal-dependent mechanism (Takahashi *et al.* 1999) suggest that orexin-containing projections to the DMV may play a key role in cephalic phase digestive responses to feeding (see Powley, 2000). In turn, the preferential targeting by central and enteric orexins of upper and lower digestive tract functions, respectively, may provide the means for co-ordinating the cephalic phase of digestion with reflex control of GI secretions and motor activity that occur upon ingestion and subsequent digestion of a meal.

Orexins modulate excitability in DMV neurones by decreasing K^+ conductance and enhancing GABAergic input

The finding that orexin-A and orexin-B depolarized a majority of gastric-projecting DMV neurones is in keeping with a number of reports in the literature that demonstrate direct excitatory effects of these peptides on central neurones, including those of the arcuate nucleus and lateral hypothalamus (van den Pol *et al.* 1998), locus coeruleus (Horvath *et al.* 1999*a*,*b*; Ivanov & Aston-Jones, 2000), tuberomammillary nucleus (Eriksson *et al.* 2001), superficial dorsal horn (Grudt *et al.* 2002), and dorsal raphe (Liu *et al.* 2002). In addition, our results largely confirm those of Hwang *et al.* (2001), who first showed that orexins produce depolarization in rat preganglionic parasympathetic vagal motor neurones via a postsynaptic mechanism. These investigators reported that the orexin-induced depolarizations and underlying inward currents resulted from the combined activation of a non-selective cation conductance and a decrease in K^+ conductance (Hwang *et al.* 2001). We also obtained evidence that orexin-A and orexin-B increase excitability by means of this combined action in some DMV neurones. However, the weight of evidence leads us to conclude that a decrease in K^+ conductance was the predominant, if not sole mechanism (in some cells) whereby activation of post-synaptic orexin receptors results in depolarization. Thus, in virtually all cases the orexin-induced depolarizations and inward currents were accompanied by an increase in membrane input resistance. Similarly, in 13 of 17 neurones examined, the steady-state *I–V* relationship for the orexin-induced inward current exhibited a decrease in slope conductance over the potential range from −120 to −50 mV and was essentially linear, implying closure of a non-voltage-gated K^+ leak conductance. For these neurones, the orexin-induced inward current showed a reversal potential of −104 ± 3.4 mV, which was close to that predicted for a pure K^+ conductance (−107 mV at 34 °C) under our normal recording conditions. Furthermore, the reversal potential for the orexin-induced current shifted in a Nernstian manner to ~ −60 mV when neurones were examined in the presence of high-K^+ Krebs solution. The finding that orexin-A did not induce changes in holding current following intracellular loading of cells with Cs^+ lends additional support to the argument that a decrease in K^+ conductance was largely responsible for the depolarization observed in a majority of gastric-projecting DMV neurones. Similar findings have recently been reported for the depolarizing actions of orexin-B (hypocretin-2) in NTS neurones (Smith *et al.* 2002). Closure of a K^+ leak conductance has also been reported to underlie orexin-induced depolarizations in neurones of the locus coeruleus (Ivanov & Aston-Jones, 2000) and dorsal raphe (Brown *et al.* 2001; but see Liu *et al.* 2002). However, this is not the only mechanism by which orexins act postsynaptically to increase excitability, as exemplified by the findings in histaminergic tuberomammillary neurones where these peptides produce depolarization via activation of both the electrogenic Na^+–Ca^{2+} exchanger and a Ca^{2+} current (Eriksson *et al.* 2001). Although we found that orexins also promoted Ca^{2+}-dependent spike discharge in DMV neurones, increased influx of Ca^{2+} ions was unlikely to contribute to the depolarizing effects of the peptides, since the latter responses were not significantly altered during blockade of Ca^{2+}-dependent events in the slice with Cd^{2+}.

In addition to having direct excitatory actions, administration of orexin-A selectively enhanced IPSCs evoked by NTS stimulation and also unmasked a bicuculline-sensitive, GABAergic outward current in a small subset of preganglionic vagal motor neurones. Interestingly, orexin-A had no effect on orthodromically evoked EPSCs, and the enhancement in inhibitory synaptic input was observed in gastric-projecting DMV neurones that did not show an excitatory response to the peptide. The orexin-induced enhancement in evoked IPSCs was accompanied by a significant change in the ratio of responses elicited by pairs of identical NTS stimuli (i.e. paired-pulse ratio), indicating that it resulted from actions of the peptide at a presynaptic site (Trombley & Westbrook, 1992; Travagli & Williams, 1996). In keeping with this, administration of orexin-A also increased the frequency and amplitude of spontaneous IPSCs in a small fraction of gastric-projecting DMV neurones. However, we did not find a significant effect of the peptide on spontaneous mIPSCs, and the bicuculline-sensitive outward currents that were unmasked by orexin-A were abolished during blockade of impulse-dependent release with TTX. Taken together, these data suggest that orexin-A may act indirectly to facilitate GABA-mediated synaptic input onto a subpopulation of gastric-projecting DMV neurones, largely by increasing the activity of NTS neurones (but see Smith *et al*. 2002). Furthermore, orexins (hypocretin-2) have recently been shown to have excitatory effects on a large percentage of neurones in caudal NTS (Smith *et al.* 2002).

Although the functional significance of this selective facilitation of synaptic inhibition is unclear, it may relate to the finding *in vivo* that microinjection of orexins into the caudal portion of the DMV evokes gastric contraction, rather than relaxation as occurs upon glutamatergic activation of neurones in this part of the nucleus (Krowicki *et al.* 2002). It should be noted in this regard that preganglionic neurones in the rostral DMV mainly synapse on to excitatory intragastric motor neurones, whereas many of those located in the caudal DMV project onto inhibitory non-adrenergic, non-cholinergic postganglionic neurones that evoke gastric relaxation (Rossiter *et al.* 1990; Takahashi & Owyang, 1997; Zheng *et al.* 1999). Nevertheless, it remains to be seen whether the facilitating effects of orexins on synaptic inhibition from NTS are differentially expressed among distinct groups of vagal motor neurones according to their specific functionality and/or their anatomical location within the DMV. Interestingly, the actions of orexins on information processing within the DMV recapitulate a pattern that occurs in the spinal cord dorsal horn (Grudt *et al.* 2002) and the dorsal raphe, where orexin-A and orexin-B modulate the activity of target neurones by producing postsynaptic excitation and also by selectively increasing inhibitory synaptic input. By contrast, orexins have been reported to inhibit synaptic transmission in the enteric nervous system, reducing the amplitude of excitatory and inhibitory postsynaptic potentials evoked in submucous plexus neurones following stimulation of interganglionic nerve bundles (Kirchgessner & Liu, 1999).

Orexins and OT excite distinct populations of vagal neurones

OT produced a slow depolarization and increased firing in a large percentage (45 %) of GI-projecting DMV neurones, confirming earlier *in vivo* results and findings in brainstem slice preparations that OT has direct stimulatory effects on preganglionic vagal motor neurones in rat (McCann & Rogers, 1990; Dubois-Dauphin *et al.* 1992; Raggenbass & Dreifuss, 1992). Dubois-Dauphin *et al.* (1992) reported that OT induced depolarization and/or generated an inward current in 78 % of a heterogeneous population of vagal motor neurones, identified in brain slice recordings by antidromic invasion following stimulation of vagal nerve fibres. We found that responsiveness to OT was expressed to a more limited extent in DMV neurones that were unambiguously defined as projecting to specific sites in the GI tract based on their retrograde labelling with DiI. This discrepancy in results could be explained if excitatory OT receptors are highly expressed in vagal neurones that supply the thoracic viscera, and many of these neurones were included in the study by Dubois-Dauphin *et al.* (1992). On the other hand, McCann & Rogers (1990) found by recording extracellularly *in vivo* in the DVC that iontophoretic administration of OT excited the vast majority (~85 %) of vagal motor neurones identified as having a gastric-related function. It could not be determined from their study to what extent the increases in cellular discharge produced by OT resulted from direct effects on the gastric-related vagal neurones themselves, or were mediated indirectly via presynaptic actions of the peptide. In this regard, OT was also found to excite virtually all (90 %) NTS neurones examined that were identified as being gastric-related (McCann & Rogers, 1990). Our results indicate that roughly half of the preganglionic vagal motor neurones that innervate the stomach express functional OT receptors and respond with postsynaptic excitation upon binding of the peptide. However, only a fraction (approximately 35%) of gastric-projecting DMV neurones that are excited by OT appear to also be responsive to the excitatory effects of orexin peptides and vice versa. Increasing the extracellular level of OT or orexin-A within the DMV, either through direct administration of peptide into the brain or via stimulation of corresponding peptide-containing inputs into the nucleus, has been shown to stimulate gastric acid secretion in rats via a vagal-dependent mechanism (Rogers & Hermann, 1985, 1987; Takahashi *et al.* 1999). Accordingly, it seems reasonable to posit that the gastric-projecting DMV neurones identified here that were excited by both orexins and OT are involved in the control of gastric acid secretion. Conversely, microinjection of orexin peptides into the DMV has been reported to stimulate gastric contraction (Krowicki *et al.* 2002), whereas direct administration of OT into the nucleus or activation of OT-containing synaptic inputs from the PVN inhibits gastric contractility and reduces basal tone (Rogers & Hermann, 1987; Flanagan *et al.* 1992). A plausible explanation for this, suggested by the present data, is that orexin- and OT-containing input to the DMV may excite functionally distinct groups of vagal motor neurones that in turn evoke gastric contraction and relaxation, respectively, through activation of cholinergic excitatory and non adrenergic, non-cholinergic inhibitory postganglionic intragastric neurones. Furthermore, blockade of central OT receptors has been reported to increase baseline gastric motility in adult rats (Flanagan *et al.* 1992), suggesting that endogenous OT may exert tonic inhibitory control over specific components of vagal efferent outflow and thus counterbalance the gastro-stimulatory effects mediated by orexin-containing input from the LH. The present results provide a cellular basis for the differential control of gastric motor function by descending orexin-containing and oxytocinergic hypothalamic projections to the DMV. Nevertheless, it remains to be determined how and to what extent these effects participate in the co-ordination of feeding behaviour and energy balance that is achieved in large part via the neuronal circuitry and projection systems of the LH and hypothalamic PVN.

REFERENCES

Bernardis LL & Bellinger L L (1996). The lateral hypothalamic area revisited: ingestive behavior. *Neurosci Biobehav Rev* **20**, 189–287.

Berthoud HR, Carlson NR & Powley TL (1991). Topography of efferent vagal innervation of the rat gastrointestinal tract. *Am J Physiol* **260**, R200–207.

Berthoud HR, Jedrzejewska A & Powley TL (1990). Simultaneous labeling of vagal innervation of the gut and afferent projections from the visceral forebrain with DiI injected into the dorsal vagal complex in the rat. *J Comp Neurol* **301**, 65–79.

Bertolino M, Vicini S, Gillis R & Travagli RA (1997). Presynaptic α2-adrenoceptors inhibit excitatory synaptic transmission in rat brain stem. *Am J Physiol* **272**, G654–661.

Brown RE, Sergeeva O, Eriksson KS & Hass HL (2001). Orexin A excites serotonergic neurons in the dorsal raphe nucleus of the rat. *Neuropharmacol* **40**, 457–459.

Browning KN, Kalyuzhny AE & Travagli RA (2002). Opioid peptides inhibit excitatory but not inhibitory synaptic transmission in the rat dorsal motor nucleus of the vagus. *J Neurosci* **22**, 2998–3004.

Browning KN, Renehan WE & Travagli RA (1999). Electrophysiological and morphological heterogeneity of rat dorsal vagal neurones which project to specific areas of the gastrointestinal tract. *J Physiol* **517**, 521–532.

Browning KN & Travagli RA (1999). Characterization of the *in vitro* effects of 5-hydroxytryptamine (5-HT) on identified neurones of the rat dorsal motor nucleus of the vagus (DMV). *Br J Pharmacol* **128**, 1307–1315.

Cai XJ, Evans ML, Lister CA, Leslie RA, Arch JjS, Wilson S & Williams G (2001). Hypoglycemia activates orexin neurons and selectively increases hypothalamic orexin-B levels: responses inhibited by feeding and possibly mediated by the nucleus of the solitary tract. *Diabetes* **50**, 105–112.

Cai XJ, Widdowson PS, Harrold J, Wilson S, Buckingham RE, Jonathan RS, Tadayyon M, Clapham JC, Wilding J & Williams G (1999). Hypothalamic orexin expression: modulation by blood glucose and feeding. *Diabetes* **48**, 2132–2137.

Date Y, Ueta Y, Yamashita H, Yamaguchi H, Matsukura S, Kangawa K, Sakurai T, Yanagisawa M & Nakazato, M. (1999). Orexins, orexigenic hypothalamic peptides, interact with autonomic, neuroendocrine and neuroregulatory systems. *Proc Natl Acad Sci U S A* **96**, 748–753.

de Lecea L, Kilduff TS, Peyron C, Gao X-B, Foye PE, Danielson PE, Fukuhara C, Battenberg ElF, Gautvik VT, Bartlett FS II, Frankel WN, van den Pol AN, Bloom FE, Gautvik KM & Sutcliffe JG (1998). The hypocretins: Hypothalamus-specific peptides with neuroexcitatory activity. *Proc Natl Acad Sci U S A* **95**, 322–327.

Dube MG, Kalra SP & Kalra PS (1999). Food intake elicited by central administration of orexins/hypocretins: identification of hypothalamic sites of action. *Brain Res* **842**, 473–477.

Dubois-Dauphin M, Raggenbass H, Widmer H, Tribollet E & Dreifuss JJ (1992). Morphological and electrophysiological evidence for postsynaptic localization of functional oxytocin receptors in the rat dorsal motor nucleus of the vagus nerve. *Brain Res* **575**, 124–131.

Eriksson KS, Sergeeva O, Brown RE & Haas HL (2001). Orexin/hypocretin excites the histaminergic neurons of the tuberomammillary nucleus. *J Neurosci* **21**, 9273–9279.

Flanagan LM, Olson BR, Sved AF, Verbalis JG & Stricker EM (1992). Gastric motility in conscious rats given oxytocin and an oxytocin antagonist centrally. *Brain Res* **578**, 256–260.

Gillis RA, Quest JA, Pagan FD & Norman WP (1989). Control centers in the central nervous system for regulating gastrointestinal motility. In *Handbook of Physiology*, section 6, *The Gastrointestinal System*, vol. 1, *Motility and Circulation*, ed. Wood JD, part 1, pp. 621–683. American Physiological Society, Bethesda, MD, USA.

Grabauskas G & Moises HC (2001). Neurons in dorsal motor nucleus of the vagus (DMV) exhibit viscerotopically organized sensitivity to hypocretins. *Soc Neurosci Abstr* **27**, 839.

Grudt TJ, van den Pol AN & Perl ER (2002). Hypocretin-2 (orexin-B) modulation of superficial dorsal horn activity in rat. *J Physiol* **538**, 517–525.

Harrison TA, Chen C-T, Dun NJ & Chang J-K (1999). Hypothalamic orexin A-immunoreactive neurons project to the rat dorsal medulla. *Neurosci Lett* **273**, 17–20.

Horvath TL, Diano S & van den Pol AN (1999*a*). Synaptic interaction between hypocretin (orexin) and neuropeptide Y cells in the rodent and primate hypothalamus: a novel circuit implicated in metabolic and endocrine regulations. *J Neurosci* **19**, 1072–1087.

Horvath TL, Peyron C, Diano S, Ivanov A, Aston-Jones G, Kilduff TS & van den Pol AN (1999*b*). Hypocretin (orexin) activation and synaptic innervation of the locus coeruleus noradrenergic system. *J Comp Neurol* **415**, 145–159.

Hwang L-L, Chen C-T & Dun NJ (2001). Mechanisms of orexin-induced depolarizations in rat dorsal motor nucleus of vagus neurones *in vitro*. *J Physiol* **537**, 511–520.

Ivanov A & Aston-Jones G (2000). Hypocretin/orexin depolarizes and decreases potassium conductance in locus coeruleus neurons. *Neuroreport* **11**, 1755–1758.

Kirchgessner AL & Liu M (1999). Orexin synthesis and response in the gut. *Neuron* **24**, 941–951.

Krowicki ZK, Burmeister MA, Berthoud H-R, Scullion RT, Fuchs K & Hornby PJ (2002). Orexins in rat dorsal motor nucleus of the vagus potently stimulate gastric motor function. *Am J Physiol* **283**, 1–15.

Krowicki ZK & Hornby PJ (1995). Hindbrain neuroactive substances controlling gastrointestinal function. In *Regulatory Mechanism in Gastrointestinal Function*, ed. Gaginella TS, pp. 277–319. CRC Press, Boca Raton, FL, USA.

Liu R-J, van den Pol AN & Aghajanian GK (2002). Hypocretins (orexins) regulate serotonin neurons in the dorsal raphe nucleus by excitatory direct and inhibitory indirect actions. *J Neurosci* **22**, 9453–9464.

Loewy AD (1990). Central autonomic pathways. In *Central Regulation of Autonomic Functions,* ed. Loewy AD & Spyer KM, pp. 88–103. Oxford University Press, New York.

Marcus JN, Aschkenasi CJ, Lee CE, Chemelli RM, Saper CB, Yanagisawa M & Elmquist JK (2001). Differential expression of orexin receptors 1 and 2 in the rat brain. *J Comp Neurol* **435**, 6–25.

McCann MJ & Rogers RC (1990). Oxytocin excites gastric-related neurones in rat dorsal vagal complex. *J Physiol* **428**, 95–108.

Naslund E, Ehrstrom M, Hellstrom PM & Kirchgessner AL (2002). Localization and effects of orexin on fasting motility in the rat duodenum. *Am J Phsyiol* **282**, G470–479.

Peyron C, Tighe DK, van den Pol AN, De Lecea L, Heller HC, Sutcliffe JG & Kilduff TS (1998). Neurons containing hypocretin (orexin) project to multiple neuronal systems. *J Neurosci* **18**, 9996–10015.

Powley TL (2000). Nutritional implications of cephalic phase responses: Vagal circuitry mediating cephalic-phase responses to food. *Appetite* **34**, 184–188.

Powley TL, Berthoud H-R, Fox EA & Laughton W (1992). The dorsal vagal complex forms a sensory-motor lattice: The circuitry of gastrointestinal reflexes. In *Neuroanatomy and Physiology of Abdominal Vagal Afferents,* ed. Ritter, RC & Barnes CD, pp. 57–79. CRC Press, Boca Raton, FL, USA.

Powley TL, Fox EA & Berthoud H-R (1987). Retrograde tracer technique for assessment of selective and total subdiaphragmatic vagotomies. *AmJ Phsyiol* **253**, R361–370.

Raggenbass M & Dreifuss JJ (1992). Mechanism of action of oxytocin in rat vagal neurones: induction of a sustained sodium-dependent current. *J Physiol* **457**, 131–142.

Rinaman L (1998). Oxytocinergic inputs to the nucleus of the solitary tract and dorsal motor nucleus of the vagus in neonatal rats. *J Comp Neurol* **399**, 101–109.

Rogers RC & Hermann GE (1985). Dorsal medullary oxytocin, vasopressin, oxytocin antagonist, and TRH effects on gastric acid secretion and heart rate. *Peptides* **6**, 1143–1148.

Rogers RC & Hermann GE (1987). Oxytocin, oxytocin antagonist, TRH, and hypothalamic paraventricular nucleus stimulation effects on gasric motility. *Peptides* **8**, 505–513.

Rossiter CD, Norman WP, Jain M, Hornby PJ, Benjamin S & Gillis RA (1990). Control of lower esophageal sphincter pressure by two sites in dorsal motor nucleus of the vagus. *Am J Physiol* **259**, G899–906.

Sakurai T, Amemiya A, Ishii M, Matsuzaki I, Chemelli RM, Tanaka H, Williams SC, Richardson JA, Kozlowski GP, Wilson S, Arch JRS, Buckingham RE, Haynes AC, Carr SA, Annan RS, McNulty DE, Liu W-S, Terrett JA, Elshourbagy NA, Bergsma DJ & Yanagisawa M (1998). Orexins and orexin receptors: a family of hypothalamic neuropeptides and G protein-coupled receptors that regulate feeding behavior. *Cell* **92**, 573–585.

Shapiro R & Miselis RR (1985). The central organization of the vagus nerve innervating the stomach of the rat. *J Comp Neurol* **238**, 473–488.

Smart D, Jerman JC, Brough SJ, Rushton SL, Murdock PR, Jewitt F, Elshourbagy NA, Ellis CE, Middlemiss DN & Brown F (1999). Characterization of recombinant human orexin receptor pharmacology in a chinese hamster ovary cell-line using FLIPR. *Br J Pharmacol* **128**, 1–3.

Smith BN, Davis SF, van den Pol AN & Xu W (2002). Selective enhancement of excitatory synaptic activity in the rat nucleus tractus solitarius by hypocretin 2. *Neuroscience* **115**, 707–714.

Sutcliffe JG & de Lecea L. (2002). The hypocretins:setting the arousal threshold. *Nature Neurosci* **3**, 339–349.

Swanson LW & Kuypers HGJM (1980). The paraventricular nucleus of the hypothalamus: cytoarchitectonic subdivision and organization of projections to the pituitary, dorsal vagal complex, and spinal cord as demonstrated by retrograde fluorescence double-labeling methods. *J Comp Neurol* **194**, 555–570.

Takahashi N, Okumura T, Yamada H & Kohgo Y (1999). Stimulation of gastric acid secretion by centrally administered orexin-A in conscious rats. *Biochem Biophys Res Comm* **254**, 623–627.

Takahashi T & Owyang C (1997). Characterization of vagal pathways mediating gastric accomodation reflex in rats. *J Physiol* **504**, 479–488.

Travagli RA, Gillis RA, Rossiter CD & Vicini S (1991). Glutamate and GABA-mediated synaptic currents in neurons of the rat dorsal motor nucleus of the vagus. *Am J Physiol* **260**, G531–536.

Travagli RA & Williams JT (1996). Endrogenous monoamines inhibit glutamate transmission in the spinal trigeminal nucleus of the guinea-pig. *J Physiol* **491**, 177–185.

Trombley PQ & Westbrook GL (1992). Excitatory synaptic transmission in cultures of rat olfactory bulb. *J Neurophysiol* **64**, 598–606.

van den Pol AN, Gao X-B, Obrietan K, Kildruff TS & Belousov AB (1998). Presynaptic and postsynaptic actions and modulation of neuroendocrine neurons by a new hypothalamic peptide, hypocretin/orexin. *J Neurosci* **18**, 7962–7971.

Willie JT, Chemelli RM, Sinton CM & Yanagisawa M. (2001). To eat or to sleep? Orexin in the regulation of feeding and wakefulness. *Annu Rev Neurosci* **24**, 429–458.

Willis A, Mihalevich M, Neff RA & Mendelowitz D (1996). Three types of postsynaptic glutamatergic receptors are activated in DMNX neurons upon stimulation of NTS. *Am J Physiol* **271**, R1614–1619.

Yamada H, Okumura T, Motomura W, Kobayashi Y & Kohgo Y (2000). Inhibition of food intake by central injection of anti-orexin antibody in fasted rats. *Biochem Biophys Res Commun* **267**, 527–531.

YamamotoY, Ueta Y, Date Y, Nakazato M, Hara Y, Serino R, Nomura M, Shibuya I, Matsukura S & Yamashita H (1999). Down regulation of the prepro-orexin gene expression in genetically obese mice. *Mol Brain Res* **65**, 14–22.

Zheng ZL, Rogers RC & Travagli RA (1999). Selective gastric projections of nitric oxide synthase-containing vagal brainstem neurons. *Neuroscience* **90**, 685–694

Zhou S, Tian D, Owyang C & Moises HC (2001). Hypocretins modulate calcium channel currents in neurones of dorsal motor nucleus of vagus (DMV). *Soc Neurosci Abstr* **24**, 503.

Acknowledgements

This work was supported by The University of Michigan GI Peptide Center Grant No. 2 P30-DK34933 and NIH grant DK061423.